AN4027
Application note

12 V - 150 W resonant converter with synchronous rectification using the L6563H, L6699 and SRK2000A

Claudio Spini

Introduction

This application note describes the EVL6699-150W-SR demonstration board features, a 12 V - 150 W converter tailored to a typical specification of an all-in-one (AIO) computer power supply or a high power adapter.

The architecture is based on a two-stage approach: a front-end PFC pre-regulator based on the L6563H TM PFC controller and a downstream LLC resonant half bridge converter using the new L6699 resonant controller. The L6699 device integrates some very innovative functions such as self-adjusting adaptive deadtime, anti-capacitive mode protection and proprietary “safe-start” procedure preventing hard switching at startup.

Thanks to the chipset used, the main features of this power supply are very high efficiency, compliant with ENERGY STAR® eligibility criteria for adapters (ENERGY STAR® rev. 2.0 for external power supplies) and with the latest ENERGY STAR® qualification criteria for computers (ENERGY STAR® ver. 6.0 for computers). The power supply also has very good efficiency at light load too and no load input power consumption is very low as well, making the board compliant with the requirements of the latest European Code of Conduct (CoC) Tier 2 and EuP Lot 6 Tier 2.

Figure 1. EVL6699-150W-SR: 150 W SMPS demonstration board

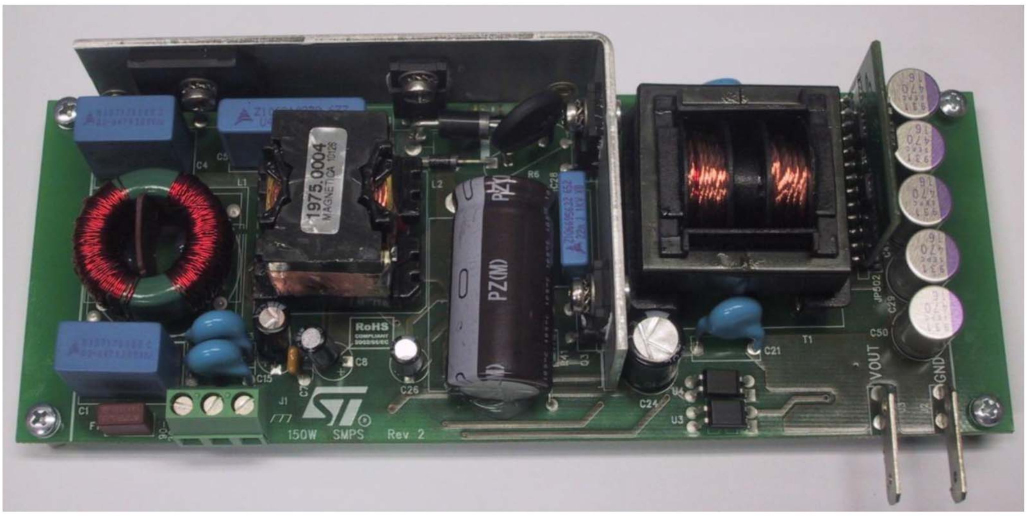

Contents

List of tables

List of figures

1 Main characteristics and circuit description

The SMPS main features are listed below:

Table 1. Main characteristics and circuit description

Parameter	Value
Input mains range	90 - 264 V_{ac} - frequency 45 to 65 Hz
Output voltage	12 V at 12.5 A continuous operation
Mains harmonics	Meets EN61000-3-2 Class-D and JEITA-MITI Class-D
No load mains consumption	< 0.15 W according to European CoC Tier 2 for external power supplies
Minimum four points average efficiency in active mode	> 89% according to European CoC Tier 2 for external power supplies
Minimum efficiency in active mode at 10 % load of full rated output current	> 79% according to European CoC Tier 2 for external power supplies
EMI	Within EN55022 Class-B limits
Safety	Meets EN60950
Dimensions	65 x 154 mm, 28 mm component maximum height
PCB	Double side, 70 µm, FR-4, mixed PTH/SMT

The circuit is made up of two stages: a front-end PFC using the L6563H, an LLC resonant converter based on the L6699, and the SRK2000A, controlling the SR MOSFETs on the secondary side. The SR driver and the rectifier MOSFETs are mounted on a daughterboard.

The L6563H is a current mode PFC controller operating in transition mode and implements a high-voltage startup to power on the converter.

The L6699 integrates all the functions necessary to properly control the resonant converter with a 50 % fixed duty cycle and working with variable frequency.

The output rectification is managed by the SRK2000A, an SR driver dedicated to LLC resonant topology.

The PFC stage works as pre-regulator and powers the resonant stage with a constant voltage of 400 V. The downstream converter operates only if the PFC is on and regulating. In this way, the resonant stage can be optimized for a narrow input voltage range.

The L6699 LINE pin (pin 7) is dedicated to this function. It is used to prevent the resonant converter from working with too low input voltage that can cause incorrect Capacitive mode operation. If the bulk voltage (PFC output) is below 380 V, the resonant startup is not allowed. The L6699 LINE pin internal comparator has a current hysteresis allowing the turn-on and turn-off voltage to be independently set. The turn-off threshold has been set to 300 V to let the resonant stage operate in the case of mains sag and consequent PFC output dip.

The transformer uses the integrated magnetic approach, incorporating the resonant series inductance. Therefore, no external, additional coil is needed for the resonance. The transformer configuration chosen for the secondary winding is center tap.

On the secondary side, the SRK2000A core function is to switch on each synchronous rectifier MOSFET whenever the corresponding transformer half-winding starts conducting (i.e. when the MOSFET body diode starts conducting) and then to switch it off when the flowing current approaches zero. For this purpose, the IC is provided with two pins (DVS1 and DVS2) sensing the MOSFETs drain voltage level.

The SRK2000A automatically detects light load operation and enters sleep mode, disabling MOSFET driving and decreasing its own consumption. This function allows great power saving at light load with respect to benchmark SR solutions.

In order to decrease the output capacitors size, aluminium solid capacitors with very low ESR were preferred to standard electrolytic ones. Therefore, high frequency output voltage ripple is limited and an output LC filter is not required. This choice allows the saving of output inductor power dissipation which can be significant in the case of high output current applications such as this.

1.1 Standby power saving

The board has a burst mode function implemented that allows power saving during light load operation.

The L6699 STBY pin (pin 5) senses the optocoupler’s collector voltage (U3), which is related to the feedback control. This signal is compared to an internal reference (1.24 V). If the voltage on the pin is lower than the reference, the IC enters an idle state and its quiescent current is reduced. As the voltage exceeds the reference by 30 mV, the controller restarts the switching. The burst mode operation load threshold can be programmed by properly choosing the resistor connecting the optocoupler to pin RFMIN (R34). Basically, R34 sets the switching frequency at which the controller enters burst mode. Since the power at which the converter enters burst mode operation heavily influences converter efficiency at light load, it must be properly set. However, despite this threshold being well set, if its tolerance is too wide, the light load efficiency of mass production converters has a considerable spread.

The main factors affecting the burst mode threshold tolerance are the control circuitry tolerances and, even more influential, the tolerances of the resonant inductance and resonant capacitor. Slight changes of resonance frequency can affect the switching frequency and, consequently, notably change the burst mode threshold. Typical production spread of these parameters, which fits the requirements of many applications, are no longer acceptable if very low power consumption in standby must be guaranteed.

As reducing production tolerance of the resonant components causes a rise in cost, a new cost-effective solution is necessary.

The key point of the proposed solution is to directly sense the output load to set the burst mode threshold. In this way the resonant elements parameters no longer affect this threshold. The implemented circuit block diagram is shown in *Figure 2*.

Figure 2. Burst-mode circuit block diagram

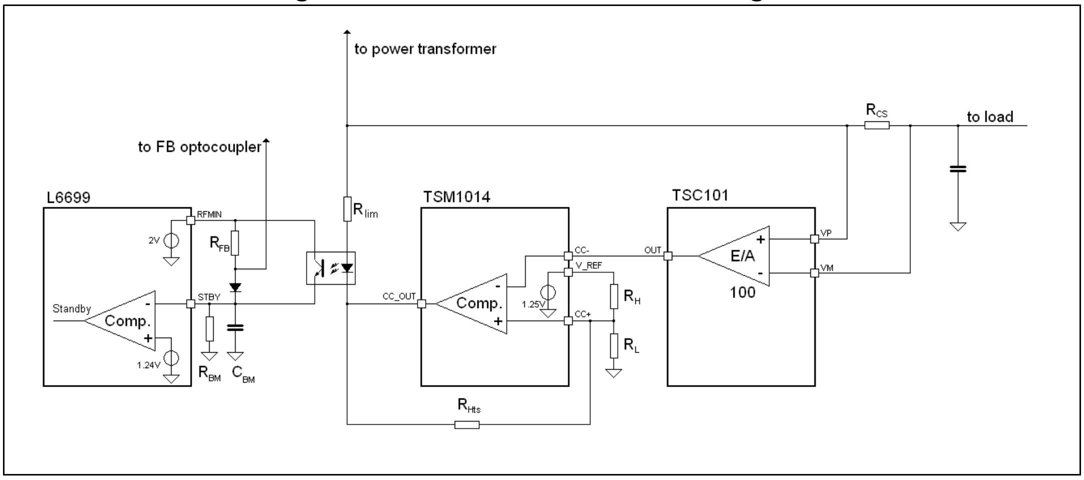

The output current is sensed by a resistor (R_{CS}); the voltage drop across this resistor is amplified by the TSC101, a dedicated high-side current sense amplifier; its output is compared to a set reference by the TSM1014; if the output load is high, the signal fed into the CC- pin is above the reference voltage, CC_OUT stays down and the optocoupler transistor pulls up the L6699 STBY pin to the RFMIN voltage (2 V), setting continuous switching operation (no burst mode); if the load decreases, the voltage on CC- falls below the set threshold, CC_OUT goes high opening the connection between RFMIN and STBY and allowing burst mode operation by the L6699. R_{CS} is dimensioned considering two constraints. The first is the maximum power dissipation allowed, based on the efficiency target. The second limitation is imposed by the need to feed a reasonable voltage signal into the TSM1014A inverting input. In fact, signals which are too small would affect system accuracy.

On this board, the maximum acceptable power dissipation has been set to $P_{loss,MAX}$ = 500 mW. R_{CS} maximum value is calculated as follows:

Equation 1

$$R_{CS,MAX} = \frac{P_{loss,MAX}}{I^2_{out,MAX}} = 3.2\text{m}\Omega$$

The burst mode threshold is set at 18 W corresponding to I_{BM} = 1.5 A output current at 12 V. Choosing V_{CC+min} = 300 mV as minimum reference of the TSM1014A, which permits a good signal to noise ratio, the R_{CS} minimum value is calculated as follows:

Equation 2

$$R_{CS,\,min} = \frac{V_{CC+min}}{100 \bullet C_{BM}} = 2\text{m}\Omega$$

The actual value of the mounted resistor is 2 mΩ, corresponding to P_{loss} = 312 mW power losses at full load. The actual resistor value at the burst mode threshold current provides an output voltage by the TSC101 of 83 mV. The reference voltage of TSM1014 V_{cc+} must be set at this level. The resistor divider setting the TSM1014 threshold R_H and R_L should be in the range of kΩ to minimize dissipation. Selecting R_L = 22 KΩ, the right R_H value is obtained as follows:

Equation 3

$$R_H = \frac{R_L(1.25V - V_{BM})}{V_{BM}} = 69.67k\Omega$$

The value of the mounted resistor is 68 kΩ.

RH sets a small debouncing hysteresis and is in the range of mega ohms. Rlim is in the range of tens of kΩ and limits the current flowing through the optocoupler's diode. Both L6699 and L6563H implement their own burst mode function but, in order to improve the power supply overall efficiency, at light load the L6699 drives the L6563H via the PFC_STOP pin and enables the PFC burst mode: as soon as the L6699 stops switching due to load drops, its PFC_STOP pin pulls down the L6563H PFC_OK pin, disabling PFC switching. Thanks to this simple circuit, the PFC is forced into idle state when the resonant stage is not switching and rapidly wakes up when the downstream converter restarts switching.

1.2 Startup sequence

The PFC acts as master and the resonant stage can operate only if the PFC output is delivering the rated output voltage. Therefore, the PFC starts first and then the LLC converter turns on. At the beginning, the L6563H is supplied by the integrated high-voltage startup circuit; as soon as the PFC starts switching, a charge pump circuit connected to the PFC inductor supplies both PFC and resonant controllers, therefore, the HV internal current source is disabled. Once both stages have been activated, the controllers are supplied also by the auxiliary winding of the resonant transformer, assuring correct supply voltage even during standby operation. As the L6563H integrated HV startup circuit is turned off, it greatly contributes to power consumption reduction when the power supply operates at light load.

1.3 L6563H brownout protection

Brownout protection prevents the circuit from working with abnormal mains levels. It is easily achieved using the RUN pin (pin 12) of the L6563H: this pin is connected through a resistor divider to the VFF pin (pin 5), which provides the information of the mains voltage peak value. An internal comparator enables the IC operations if the mains level is correct, within the nominal limits. At startup, if the input voltage is below 90 V_{ac} (typ.), circuit operations are inhibited.

1.4 L6563H fast voltage feed-forward

The voltage on the L6563H VFF pin (pin 5) is the peak value of the voltage on the MULT pin (pin 3). The RC network (R15 + R26, C12) connected to VFF completes a peak-holding circuit. This signal is necessary to derive information from the RMS input voltage to compensate the loop gain that is mains voltage dependent.

Generally speaking, if the time constant is too small, the voltage generated is affected by a considerable amount of ripple at twice the mains frequency, therefore causing distortion of the current reference (resulting in higher THD and lower PF). If the time constant is too large, there is a considerable delay in setting the right amount of feed-forward, resulting in excessive overshoot or undershoot of the pre-regulator's output voltage in response to large line voltage changes.

To overcome this issue, the L6563H device implements the fast voltage feed-forward function. As soon as the voltage on the VFF pin decreases by a set threshold (40 mV typically), a mains dip is assumed and an internal switch rapidly discharges the VFF capacitor via a 10 kΩ resistor. Thanks to this feature, it is possible to set an RC circuit with a long time constant, assuring a low THD, keeping a fast response to mains dip.

1.5 L6699 overload and short-circuit protection

The current into the primary winding is sensed by the lossless circuit R41, C27, R78, R79, and C25 and it is fed into the ISEN pin (pin 6). In the case of overload, the voltage on the pin surpasses an internal threshold (0.8 V) that triggers a protection sequence. An internal switch is turned on for 5 µs and discharges the soft-start capacitor C18. This quickly increases the oscillator frequency and thereby limits energy transfer. Under output short-circuit conditions, this operation results in a peak primary current that periodically oscillates below the maximum value allowed by the sense resistor R78.

The converter runs under this condition for a time set by the capacitor (C45) on pin DELAY (pin 2). During this condition, C45 is charged by an internal 150 µA current generator and is slowly discharged by the external resistor (R24). If the voltage on the pin reaches 2 V, the soft-start capacitor is completely discharged so that the switching frequency is pushed to its maximum value. As the voltage on the pin exceeds 3.5 V, the IC stops switching and the internal generator is turned off, so that the voltage on the pin decays because of the external resistor. The IC is soft-restarted as the voltage drops below 0.3 V. In this way, under short-circuit conditions, the converter works intermittently with very low input average power.

This procedure allows the converter to handle an overload condition for a time lasting less than a set value, avoiding IC shutdown in the case of short overload or peak power transients. On the other hand, in the case of dead short, a second comparator referenced to 1.5 V immediately disables switching and activates a restart procedure.

1.6 L6699 anti-capacitive protection

The LLC resonant half bridge converter must operate with the resonant tank current lagging behind the square-wave voltage applied by the half bridge leg. This is a necessary condition in order to obtain correct soft switching by the half bridge MOSFETs. If the phase relationship reverses, i.e. the resonant tank current leads the applied voltage, like in circuits having a capacitive reactance, soft switching is lost. This condition is called capacitive mode and must be avoided because of significant drawbacks coming from hard switching (refer to the L6699 datasheet).

Resonant converters work in capacitive mode when their switching frequency falls below a critical value that depends on the loading conditions and the input-to-output voltage ratio. They are especially prone to run in capacitive mode when the input voltage is lower than the minimum specified and/or the output is overloaded or short-circuited. Designing a converter so that it never works in capacitive mode, even under abnormal operating conditions, is certainly possible but this may pose unacceptable design constraints in some cases.

To prevent the severe drawbacks of capacitive mode operation, while enabling a design that needs to ensure Inductive mode operation only in the specified operating range, neglecting abnormal operating conditions, the L6699 provides the capacitive mode detection function. The IC monitors the phase relationship between the tank current circuit sensed on the ISEN pin and the voltage applied to the tank circuit by the half bridge, checking that the former lags behind the latter (Inductive mode operation). If the phase shift approaches zero, which is indicative of impending capacitive mode operation, the monitoring circuit activates the overload procedure described above so that the resulting frequency rise keeps the converter away from that dangerous condition. Also in this case, the DELAY pin is activated, so that the OLP function, if used, is eventually tripped after a time TSH causing intermittent operation and reducing thermal stress.

If the phase relationship reverses abruptly (which may happen in the case of dead short at the converter's output), the L6699 is stopped immediately, the soft-start capacitor C18 is totally discharged and a new soft-start cycle is initiated after 50 µs idle time. During this idle period the PFC_STOP pin is pulled low to stop the PFC stage as well.

1.7 Output voltage feedback loop

The feedback loop is implemented by means of a typical circuit using the dedicated operational amplifier of the TSM1014A modulating the current in the optocoupler diode. The second operational amplifier embedded in the TSM1014A, usually dedicated to constant current regulation, is here utilized for burst mode as previously described.

On the primary side, R34 and D17 connect the RFMIN pin (pin 4) to the optocoupler's photo transistor closing the feedback loop. R31, which connects the same pin to ground, sets the minimum switching frequency. The RC series R44 and C18 sets both soft-start maximum frequency and duration.

1.8 Open loop protection

Both circuit stages, PFC and resonant, are equipped with their own overvoltage protection. The PFC controller L6563H monitors its output voltage via the resistor divider connected to a dedicated pin (PFC_OK, pin 7) protecting the circuit in case of loop failures or disconnection. If a fault condition is detected, the internal circuitry latches the L6563H operations and, by means of the PWM_LATCH pin (pin 8), it latches the L6699 as well via the DIS pin (pin 8). The converter is kept latched by the L6563H internal HV startup circuit that supplies the IC by charging the V_{CC} capacitor periodically. To resume converter operation, mains restart is necessary. The LLC open loop protection is realized by monitoring the output voltage through sensing the V_{CC} voltage. If V_{CC} voltage overrides the D12 breakdown voltage, Q9 pulls down the L6563H INV pin latching the converter. Even in this case, to resume converter operation, mains restart is necessary.

Figure 3. Electrical diagram

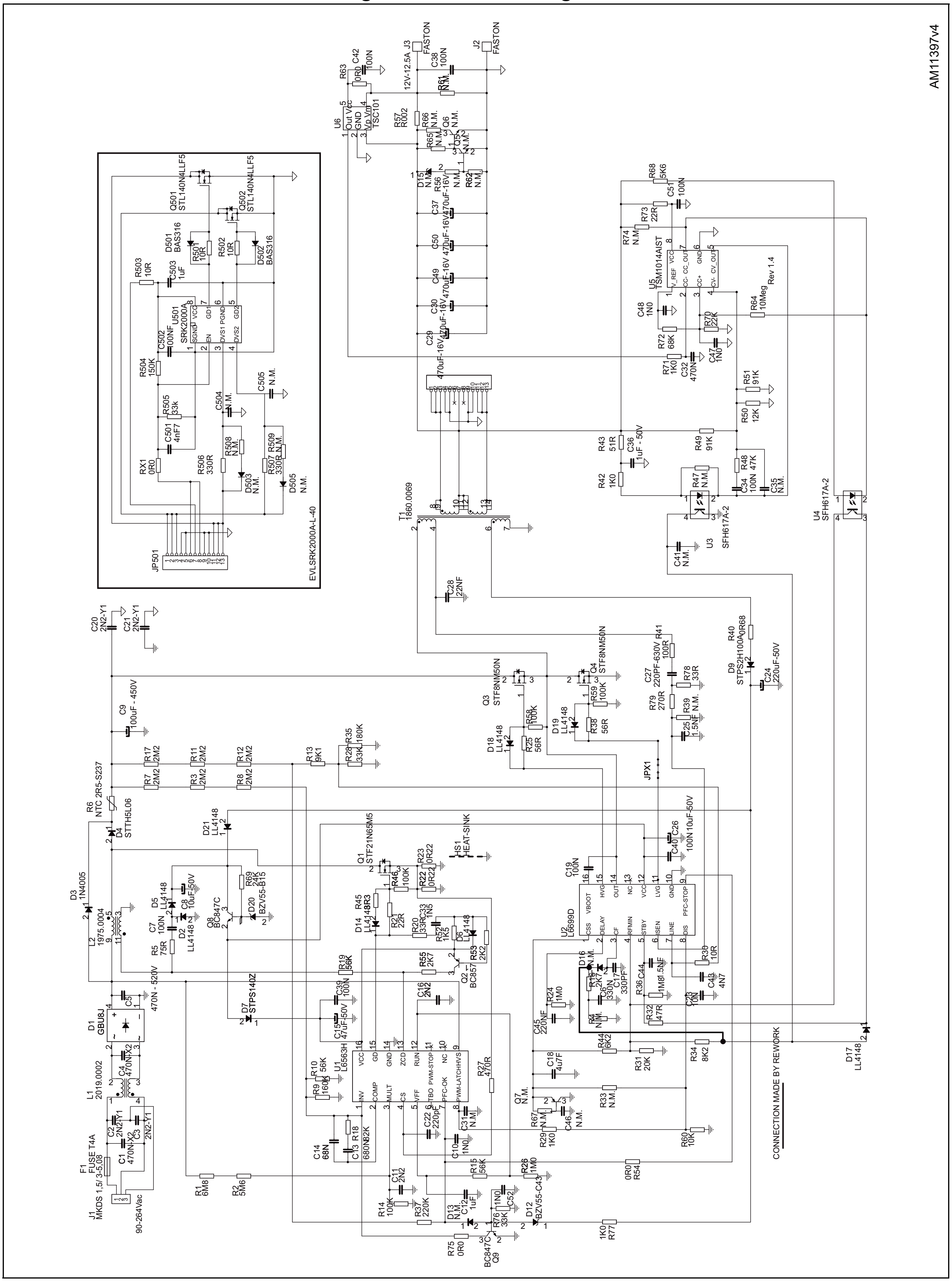

2 Efficiency measurements

Table 2 shows the no load consumption and the overall efficiency measurements at the nominal mains voltages. At 115 V_{ac} the full load efficiency is 91.5%, and at 230 V_{ac} it is 93.2%, which are both high values for a double stage power supply and confirm the benefit of implementing the synchronous rectification. The results are also shown in *Figure 5* as a graph.

Also at no load, the board performance is superior for a 150 W power supply: no load consumption at nominal mains voltage is lower than 160 mW.

Table 2. Efficiency measurements

Input voltage	Load condition	Vout [V]	Iout [A]	Pout [W]	Pin [W]	Efficiency (%)
115 V - 60 Hz	No load	12.00	0.00	0.00	0.132	-
	10%	11.99	1.257	15.07	18.04	83.54
	20%	11.99	2.50	29.98	35.58	84.2
	25%	11.99	3.13	37.53	43.36	86.6
	50%	11.97	6.25	74.81	82.53	90.6
	75%	11.96	9.38	112.18	122.54	91.5
	100%	11.94	12.50	149.25	163.12	91.5
230 V - 50 Hz	No load	12.00	0.00	0.00	0.145	-
	10%	11.98	1.258	15.07	17.43	86.46
	20%	11.99	2.50	29.98	35.35	84.8
	25%	11.98	3.14	37.62	43.27	86.9
	50%	11.97	6.25	74.81	81.56	91.7
	75%	11.96	9.38	112.18	120.66	93.0
	100%	11.94	12.50	149.25	160.22	93.2

Figure 4. Graph of efficiency measurements

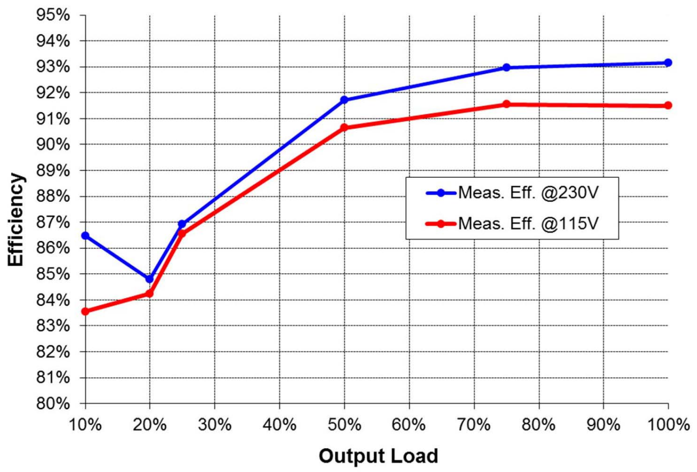

2.1 ENERGY STAR® for external power supplies ver. 2.0 compliance verification

In *Table 3* the comparison between the regulation requirements and the test results are reported: note that the design overcomes the requirements with margin. The average efficiency is measured at 25 %, 50 %, 75 %, 100 % load, the no load input power consumption and the power factor at full load meet these regulation requirements for adapters.

Table 3. European CoC Tier 2 and ENERGY STAR® ver. 2.0 for external power supplies compliance verification

European CoC Tier 2 and ENERGY STAR® ver. 2.0 requirements for external power supplies	Test results		Limits	Status
	115 V_{ac} - 60 Hz	230 V_{ac} - 50 Hz		
Average efficiency 25 %, 50 %, 75 %, 100 % load	0.901	0.912	> 0.87	Pass
Efficiency at 10% load	0.835	0.865	> 0.79	
No load input power [W]	0.132 W	0.145 W	< 0.15 W	
Power factor	0.991	0.972	> 0.9	

2.2 ENERGY STAR® for computers ver. 6.0 compliance verification

Because the EVL6699-150W-SR design is suitable to power even all-in-one computers, having to meet the ENERGY STAR® regulation for computers, the test results have been compared with the latest ver. 6.0 requirements of this document. In the comparison between the regulation requirements and the test results are reported: note that, in this case the efficiency limit is not the average efficiency measured at different loads but there are three different values of minimum efficiency to be met, at 20 %, 50 %, and 100 % load. Even in this case, at full load the minimum power factor must be 0.9 minimum. In all load and line conditions the EVL6699-150W-SR has efficiency and power factor much better than the minimum required by the ENERGY STAR® regulation.

Table 4. ENERGY STAR® for computers ver. 6.0 compliance verification

ENERGY STAR® requirements for computers ver. 6.0:	Test results		Limits	Status
	115 V_{ac} - 60 Hz	230 V_{ac} - 50 Hz		
Efficiency at 20 % load	0.842	0.848	> 0.82	Pass
Efficiency at 50 % load	0.906	0.917	> 0.85	
Efficiency at 100 % load	0.915	0.932	> 0.82	
Power factor	0.991	0.972	> 0.9	

2.3 Light load operation efficiency

Computer power supplies must now meet higher efficiency limits than in the past even at light load because, according to latest regulations such as the EuP Ecodesign requirements for household and office equipment Lot 6 Tier 2, the maximum power consumption during computer standby and off mode has decreased.

Measurement results are reported in *Table 4* and plotted in *Figure 5*. As seen, efficiency is better than 50% even for very light loads such as 250 mW. This high efficiency at light load allows the board to meet also the regulation of the low power status ENERGY STAR® program for computers ver. 5.0.

Measurement procedure:

1. Because the current flowing through the circuit under measurement is relatively small, the current measurement circuit is connected to the demonstration board side and the voltage measurement circuit is connected to the AC source side. In this way, the current absorbed by the voltage circuit is not considered in the measured consumption amount.
2. During any efficiency measurement, remove any oscilloscope probe from the board.
3. For any measurement load, apply a warm-up time of 20 minutes by each different load. Loads have been applied increasing the output power from minimum to maximum.
4. Because of the input current shape during light load condition, the input power measurement may be critical or unreliable using a power meter in the usual way. To overcome this issue, all light measurements have been done by measuring the active energy consumption of the demonstration board under test and then calculating the power as the energy divided by the integration time. The integration time has been set to 36 seconds, as a compromise between a reliable measurement and a reasonable time measurement time. The energy is measured in mWh, the result in mW is then simply calculated by dividing the instrument reading (in mWh) by 100. The instrument used was the Yokogawa, WT210 power meter.

Table 5. Light load efficiency

Test	230 V - 50 Hz					115 V - 60 Hz				
	Vout [V]	Iout [mA]	Pout [W]	Pin [W]	Eff. [%]	Vout [V]	Iout [mA]	Pout [W]	Pin [W]	Eff. [%]
0.25 W	12.00	10.40	0.125	0.319	39.1	12.00	10.40	0.125	0.310	40.3
0.5 W	12.00	20.90	0.251	0.473	53.0	12.00	20.90	0.251	0.471	53.2
1.0 W	12.00	41.68	0.500	0.768	65.1	12.00	41.68	0.500	0.785	63.7
1.5 W	12.00	83.50	1.002	1.358	73.8	12.00	83.50	1.002	1.415	70.8
2.0 W	12.00	125.03	1.500	1.940	77.3	12.00	125.03	1.500	2.045	73.4
2.5 W	12.00	167.09	2.005	2.525	79.4	12.00	166.84	2.002	2.651	75.5
3.0W	12.00	209.09	2.509	3.112	80.6	12.00	208.56	2.503	3.267	76.6
3.5 W	12.00	250.37	3.004	3.687	81.5	12.00	250.09	3.001	3.867	77.6
4.0 W	12.00	291.65	3.500	4.260	82.2	12.00	292.02	3.504	4.479	78.2

Table 5. Light load efficiency (continued)

Test	230 V - 50 Hz					115 V - 60 Hz				
	Vout [V]	Iout [mA]	Pout [W]	Pin [W]	Eff. [%]	Vout [V]	Iout [mA]	Pout [W]	Pin [W]	Eff. [%]
4.5 W	12.00	333.65	4.004	4.844	82.7	12.00	333.65	4.004	5.090	78.7
5.0 W	12.00	375.43	4.505	5.423	83.1	12.00	375.65	4.508	5.683	79.3

Figure 5. Light load efficiency diagram

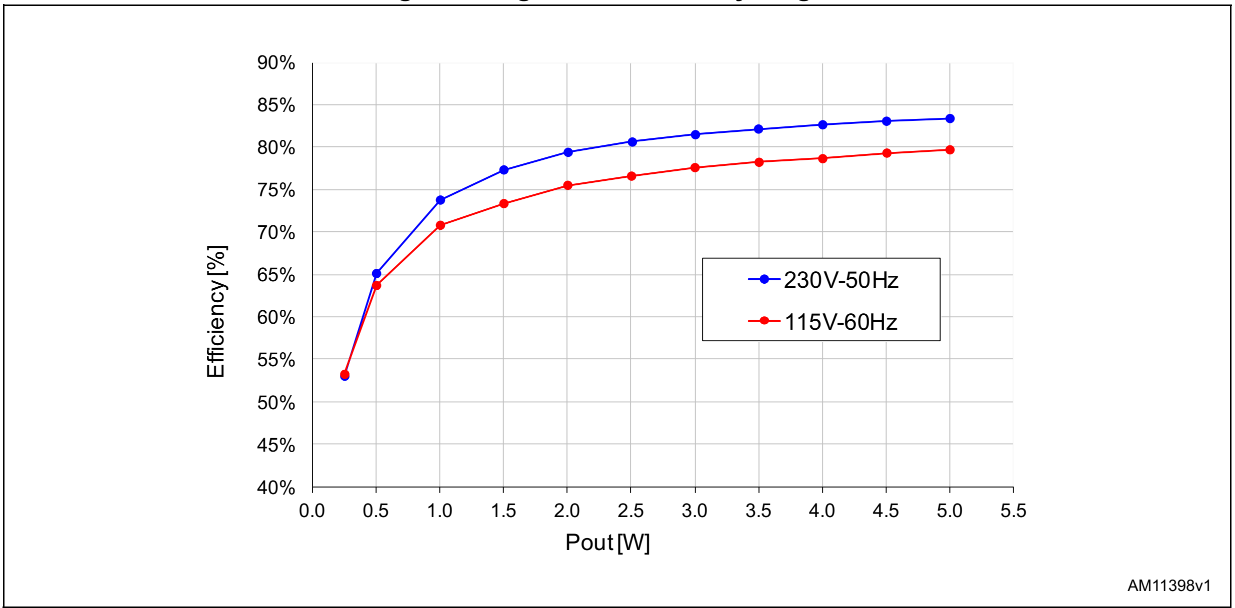

3 Harmonic content measurement

The board has been tested according to the European Standard EN61000-3-2 Class-D and Japanese standard JEITA-MITI Class-D, at both the nominal input voltage mains. As reported in the following figures, the circuit is able to reduce the harmonics well below the limits of both regulations.

On the bottom side of the diagrams the total harmonic distortion and power factor have been measured too. The values in all conditions give a clear idea about the correct functionality of the PFC.

Figure 6. Compliance to EN61000-3-2 at 230 V_{ac} - 50 Hz, full load

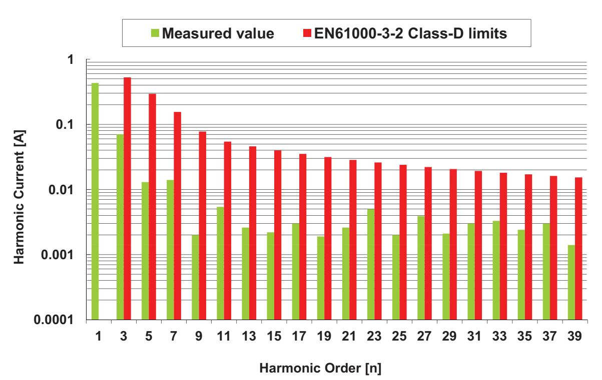

THD: 18.2 % - PF = 0.972

AM11399v1

Figure 7. Compliance to JEITA-MITI at 100 V_{ac} - 50 Hz, full load

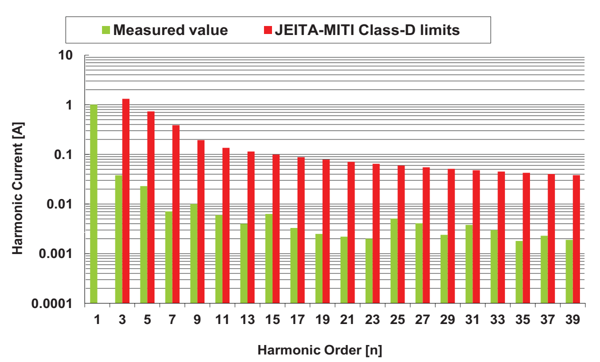

THD: 7.5 % - PF = 0.933

AM11400v1

In *Figure 7* and *Figure 8* the input mains current is shown at both nominal mains input voltages, European and Japanese. At European mains the waveforms show a slightly higher THD value because, in order to increase the efficiency, the PFC switching frequency is limited to a value around 125 kHz. However, all harmonics are within the limits specified by both regulations.

Figure 8. Mains voltage and current waveforms at 230 V - 50 Hz - full load

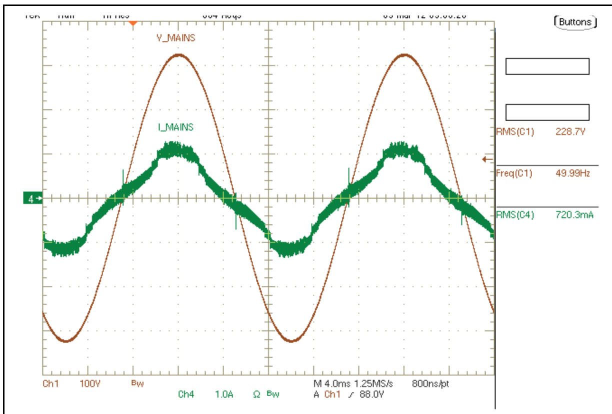

CH1: Mains voltage
CH2: Mains current

AM11401v1

Figure 9. Mains voltage and current waveforms at 100 V - 50 Hz - full load

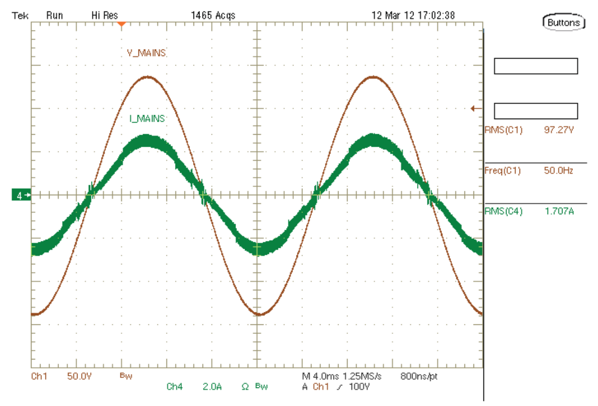

CH1: Mains voltage
CH2: Mains current

AM11402v1

4 Functional check

In *Figure 10* some waveforms relevant to the resonant stage during steady-state operation are reported. The selected switching frequency is about 120 kHz, in order to have a good trade-off between transformer losses and dimensions. The converter operates slightly above the resonance frequency. *Figure 11* shows key signals of the SRK2000A: each rectifier MOSFET is switched on and off according to its drain-source voltage which, during conduction time, is the voltage of the current flowing through the MOSFET.

Figure 10. Resonant stage waveforms at 115 V_{ac} - 60 Hz - full load

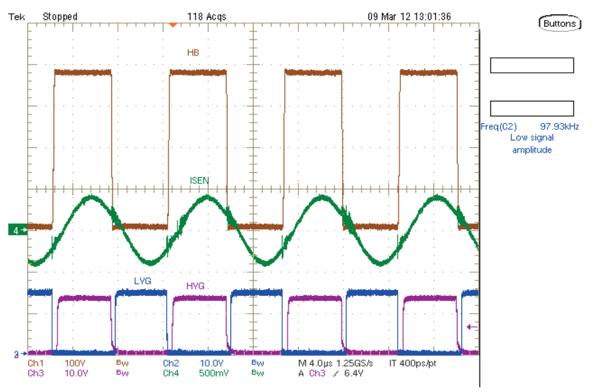

CH1: HB voltage CH2: LVG pin voltage
CH3: HVG pin voltage CH4: ISEN pin voltage AM11403v1

Figure 11. SRK2000A key signals at 115 V_{ac} - 60 Hz - full load

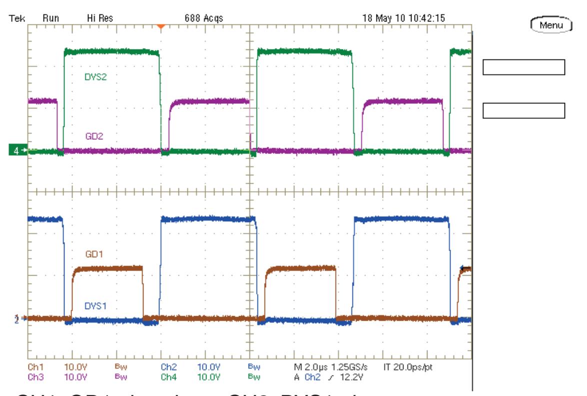

CH1: GD1 pin voltage CH2: DVS1 pin
CH3: GD2 pin voltage CH4: DVS2 pin AM11404v1

A peculiarity of the L6699 is the self-adaptive deadtime, modulated by the internal logic according to the half bridge node transition time. This feature allows the maximization of the transformer magnetizing inductance, therefore obtaining good light load efficiency and also keeping correct operation by the HB. *Figure 12* and *Figure 13* show the waveforms during full load operation. It is possible to note the measurement of the edges and the relevant deadtime.

Figure 12. HB transition at full load - rising edge

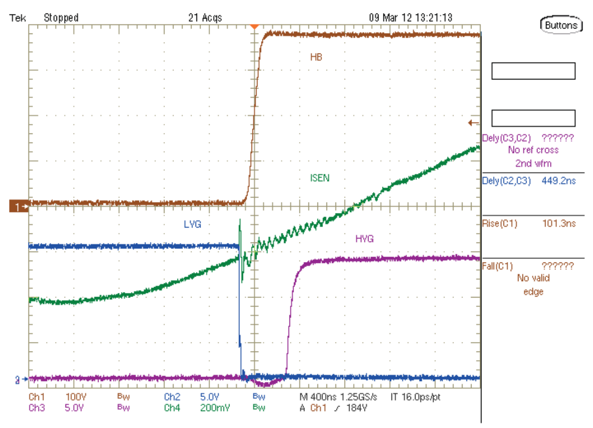

CH1: HB voltage CH2: LVG
CH3: HVG CH4: ISEN pin voltage AM11405v1

Figure 13. HB transition at full load - falling edge

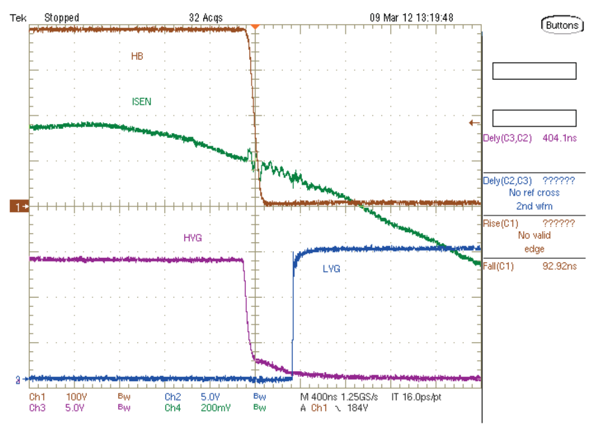

CH1: HB voltage CH2: LVG
CH3: HVG CH4: ISEN pin voltage AM11406v1

In *Figure 14* and *Figure 15* the same images are captured during light load operation: note that because of the resonant tank parameters, the half bridge transitions have similar rise and fall times because the switched current is almost the same value in both load conditions. In this case, the L6699 does not appreciably change the deadtime. In all conditions it can be noted that both MOSFETs are turned on while resonant current is flowing through their body diodes and drain-source voltage is zero, therefore achieving the MOSFETs ZVS operation at turn-on.

Figure 14. HB transition at 0.25 A - rising edge

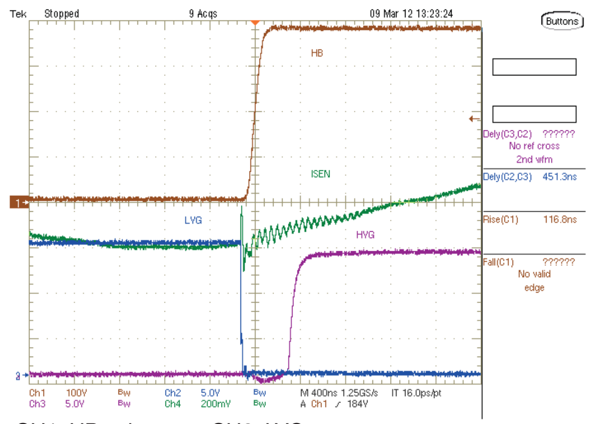

CH1: HB voltage CH2: LVG
CH3: HVG CH4: ISEN pin voltage
AM11407v1

Figure 15. HB transition at 0.25 A - falling edge

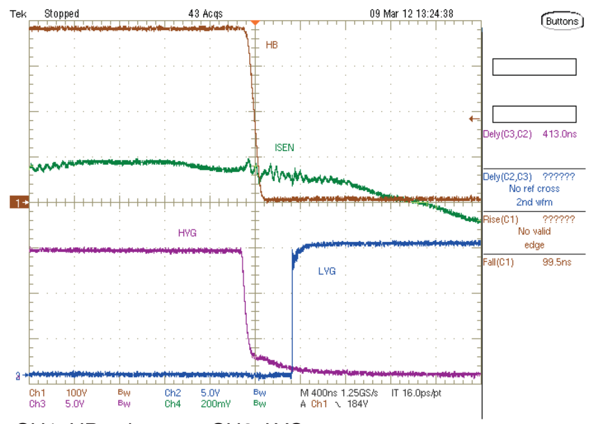

CH1: HB voltage CH2: LVG
CH3: HVG CH4: ISEN pin voltage
AM11408v1

Figure 16. L6699 pin signals-1

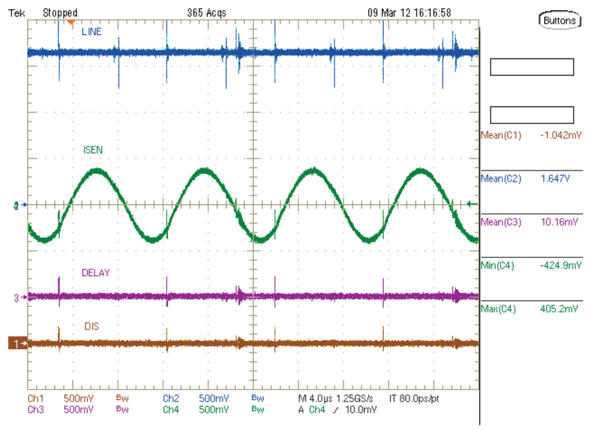

CH1: DIS CH2: LINE
CH3: DELAY CH4: ISEN
AM11409v1

Figure 17. L6699 pin signals-2

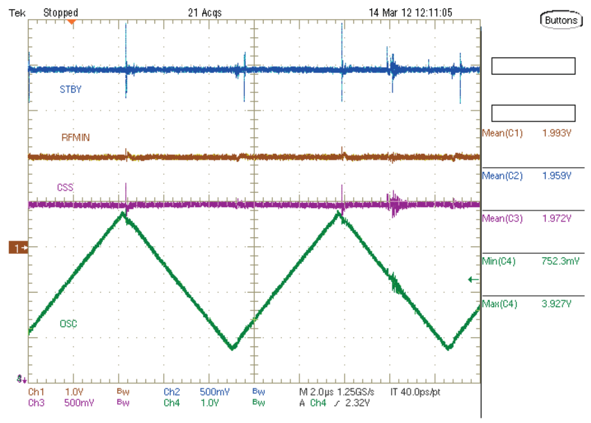

CH1: RFmin CH2: STBY
CH3: CSS CH4: CF
AM11410v1

In *Figure 16* some signals at L6699 pins are measured. It can be seen that the signal on the ISEN pin (#6) matches the instantaneous current flowing in the transformer primary side. Contrary to the former resonant controllers such as the L6599A and others, requiring an integration of current signal, the L6699 integrates the anti-capacitive mode protection, therefore it needs to sense the instantaneous value of the current in order to check the phase between the voltage and current. The LINE pin (#7) has been dimensioned to start up the L6699 once the PFC output voltage has reached the rated value, in order to have correct converter sequencing, with PFC starting first and LLC starting later in order to optimize the design of the LLC converter and prevent capacitive mode operation that may occur because of operation at too low input voltage.

The DELAY pin (#2) is zero, as it must be during normal operation, because it works during the overcurrent protection operation. The DIS pin (#8) is used for open loop protection and therefore, even in this case, its voltage is at ground level.

In *Figure 17* the pin voltages relevant to the control part of the L6699 are reported: the RFmin pin (#4) is a 2 V (typ.) reference voltage of the oscillator, the switching frequency is proportional to the current flowing out from the pin. CSS pin (#1) voltage is the same value as pin #4 because it is connected to the latter via a resistor (R44), determining the soft-start frequency. A capacitor (C18) is also connected between the CSS pin and ground, to set the soft-start time. At the beginning of L6699 operation the voltage on the CSS pin is at ground level because C18 is discharged, then the CSS pin (#1) voltage increases according to the time constant till the RFmin voltage level is reached. The STBY pin (#5) senses the optocoupler voltage; once the voltage decreases to 1.25 V, both gate drivers stop switching and the circuit works in burst mode. The CF pin (#3) is the controller oscillator; its ramp speed is proportional to the current flowing out from the RFmin pin (#4). The CF signal must be clean and undistorted to obtain correct symmetry by the half bridge current, and therefore care must be taken in the layout of the PCB.

4.1 Startup

The waveforms relevant to the board startup at 90 V_{ac} and full load have been captured in *Figure 18*. Note that the output voltage reaches the nominal value approximately 800 ms after plug-in. The L6563H, HV PFC controller, has an embedded high-voltage startup charging the V_{cc} capacitor by a constant current, ensuring a constant wake-up time. This can be seen by comparing *Figure 18* with *Figure 19*, relevant to a startup at 265 V_{ac} and no load, the output voltage rises at the nominal level in the same time. In both conditions the output voltage has no overshoot or dips.

Figure 18. Startup at 90 V_{ac} - full load

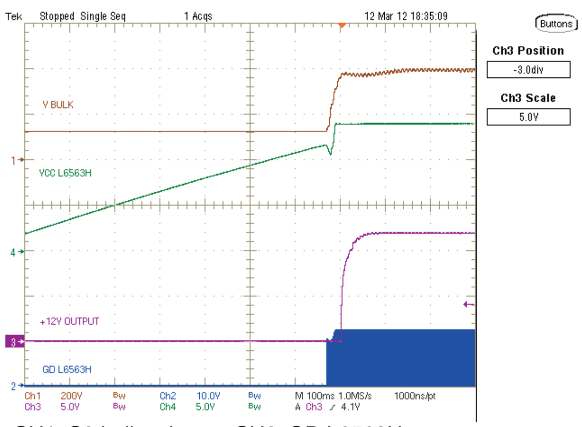

CH1: C9 bulk voltage CH2: GD L6563H
CH3: +12 Vout CH4: VCC L6563H
AM11411v1

Figure 19. Startup at 265 V_{ac} - no load

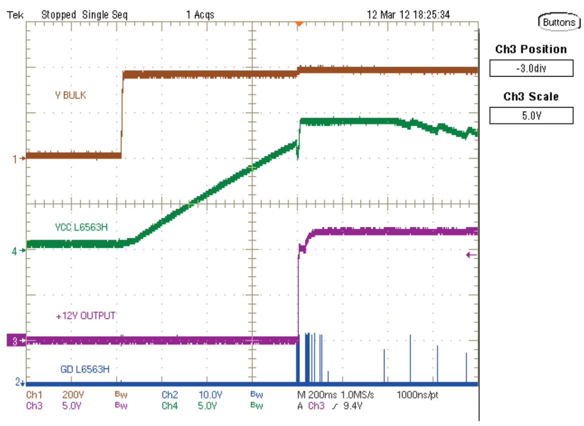

CH1: C9 bulk voltage CH2: GD L6563H
CH3: +12 Vout CH4: VCC L6563H
AM11412v1

In *Figure 20* the salient waveforms in the resonant tank during start up of the LLC are reported. In *Figure 21* the detail of waveforms at the beginning of operation shows that the resonant circuit is working correctly in zero voltage switching operation from the initial cycles. In the L6699 a new startup procedure, called “safe-start”, has been implemented in order to prevent loss of soft-switching during the initial switching cycles which typically is not guaranteed by the usual soft-start procedure. At startup, the voltage across the resonant capacitor is often quite different from Vin/2, as during normal steady-state operation, so it takes some time for its DC component to reach the steady-state value Vin/2. During this transient, the transformer is not driven symmetrically and there is a significant V · s imbalance in two consecutive half-cycles. If this imbalance is large, there is a significant difference in the up and down slopes of the tank current and, in a typical controller working with fixed 50% duty cycle, as the duration of the two half-cycles is the same, the current may not reverse in a switching half-cycle. Therefore, one MOSFET can be turned on while the body diode of the other is conducting and this may happen for a few cycles. To prevent this, the L6699 is provided with a proprietary circuit that modifies the normal operation of the oscillator during the initial switching cycles, so that the initial V · s unbalance is almost eliminated. Its operation is such that current reversal in every switching half-cycle and, then, soft-switching, is ensured. In *Figure 21* it can be noted that at the beginning of operation the duty cycle of the half bridge is initially considerably less than 50%, the tank current has lower peak values and changes sign every half-cycle, while the DC voltage across the resonant capacitor reaches the steady-state. The device goes to normal operation after approximately 50 µs from the first switching cycle. This transition is almost seamless and just a small perturbation of the tank current can be observed.

Figure 20. Startup at 115 V_{ac} - full load

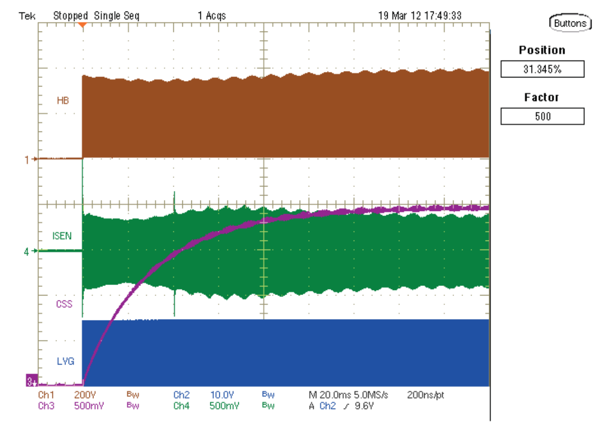

CH1: HB voltage CH2: LVG
CH3: CSS CH4: ISEN
AM11413v1

Figure 21. Startup at full load - detail

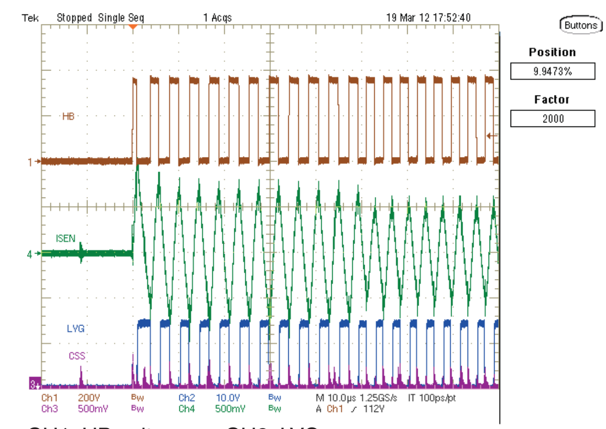

CH1: HB voltage CH2: LVG
CH3: CSS CH4: ISEN
AM11414v1

4.2 Burst mode operation at light load

In *Figure 22* some burst mode pulses are captured during 250 mW load operation. The burst pulses are very narrow and their period is quite long, therefore the resulting equivalent switching frequency is very low, ensuring high efficiency. The resulting output voltage ripple during burst mode operation is about 200 mV peak-to-peak.

In *Figure 23* the detail of the burst is reported: the first initial pulse is shorter than the following ones avoiding the typical high current peak at half bridge operation restarting, due to the recharging or the resonant capacitor. The maximum operating frequency of the half bridge, set by the resistor R34 in series to the optocoupler, is around 77 kHz.

Figure 22. Pout = 250 mW operation

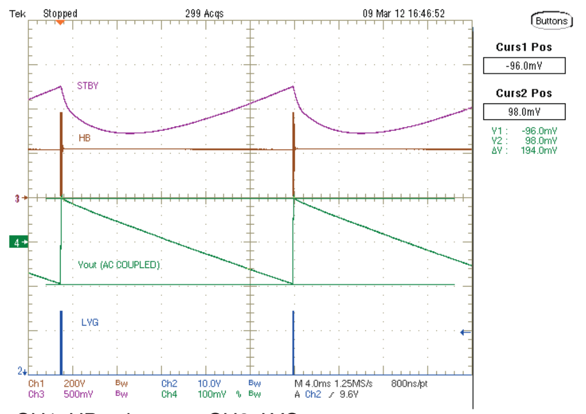

CH1: HB voltage CH2: LVG
CH3: STBY CH4: Vout (AC coupl.)
AM11624v1

Figure 23. Pout = 250 mW operation - detail

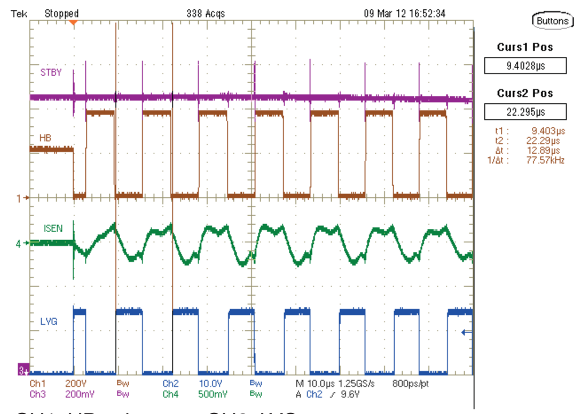

CH1: HB voltage CH2: LVG
CH3: STBY CH4: Res. tank current
AM11625v1

In *Figure 24* and *Figure 25* the transitions from full load to no load and vice versa have been checked. As seen in the images, both transitions are clean and there isn't any output voltage dip.

Figure 24. Transition full load to no load at 115 V_{ac} - 60 Hz

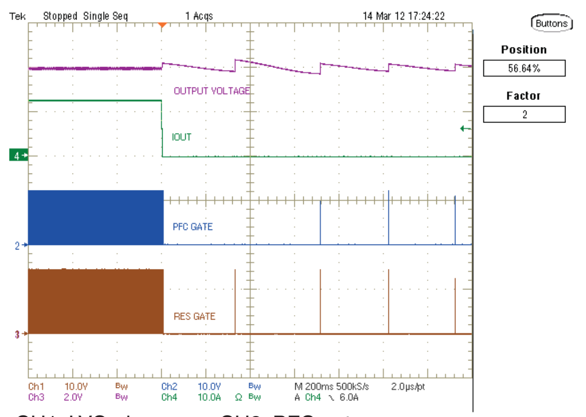

CH1: LVG pin CH2: PFC gate
CH3: Output voltage CH4: Output current
AM11626v1

Figure 25. Transition no load to full load at 115 V_{ac} - 60 Hz

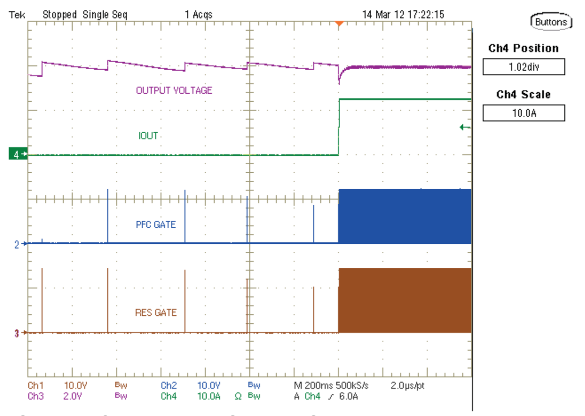

CH1: LVG pin CH2: PFC gate
CH3: Output voltage CH4: Output current
AM11627v1

4.3 Overcurrent and short-circuit protection

The L6699 is equipped with a current sensing input (pin 6, ISEN) and a dedicated overcurrent management system. The current flowing in the resonant tank is detected and the signal is fed into the ISEN pin. It is internally connected to a first comparator, referenced to 0.8 V, and to a second comparator referenced to 1.5 V. If the voltage externally applied to the pin exceeds 0.8 V, the first comparator is tripped causing an internal switch to be turned on and to discharge the soft-start capacitor CSS.

Under output short-circuit, this operation results in a nearly constant peak primary current. With the L6699, the board designer can externally program the maximum time that the converter is allowed to run overloaded or under short-circuit conditions. Overloads or short-circuits lasting less than the set time do not cause any other action, therefore providing the system with immunity to short duration phenomena. If, instead, the overload condition keeps going, a protection procedure is activated that shuts down the L6699 and, in the case of continuous overload/short-circuit, results in continuous intermittent operation with a user defined duty cycle. This function is realized with the DELAY pin (pin 2), by means of a capacitor C45 and the parallel resistor R24 connected to ground. As the voltage on the ISEN pin exceeds 0.8 V, the first OCP comparator, in addition to discharging CSS, turns on an internal 150 µA current generator that, via the DELAY pin, charges C45. When the voltage on C45 is 3.5 V, the L6699 stops switching and the PFC_STOP pin is pulled low. Also the internal generator is turned off, so that C45 is now slowly discharged by R24. The IC restarts when the voltage on C45 becomes lower than 0.3 V.

Additionally, if the voltage on the ISEN pin reaches 1.5 V for any reason (e.g. transformer saturation), the second comparator is triggered, the L6699 shuts down and C45 is charged to 3.5 V. Even in this case, the operation is resumed once the voltage on C45 drops below 0.3 V.

In *Figure 26* a dead short-circuit event has been captured. In this case the overcurrent protection is triggered by the second comparator referenced at 1.5 V which immediately stops switching by the L6699 and discharging of the soft-start capacitor; at the same time the capacitor connected to the DELAY pin (#2) begins charging up to 3.5 V (typ.). Once the voltage on the DELAY pin reaches 3.5 V, the L6699 stops charging the delay capacitor (C45) and the L6699 operation is resumed once the DELAY pin (#2) voltage decays to 0.3 V (typ.) by the parallel resistor (R24), via a soft-start cycle. If the short-circuit condition is removed, the converter again starts operation, otherwise if the short is still there, the converter operation results in an intermittent operation (Hiccup mode) with a narrow operating duty cycle of the converter, in order to prevent overheating of power components, as can be noted in *Figure 28*.

In *Figure 27* details of peak current with short-circuit occurring is shown. It is possible to see the ZVS correct operation by the half bridge MOSFETs.

Figure 26. Short-circuit at full load

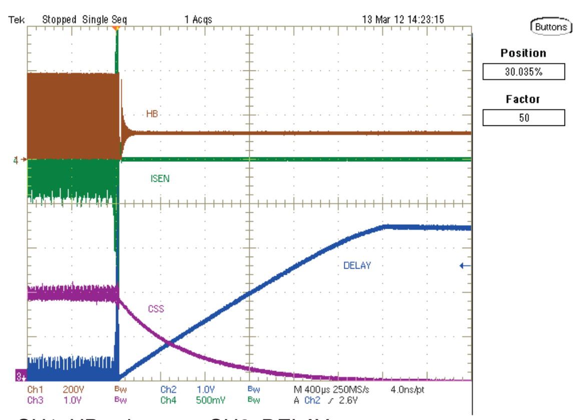

CH1: HB voltage CH2: DELAY
CH3: CSS CH4: ISEN
AM11628v1

Figure 27. Short-circuit at full load – detail

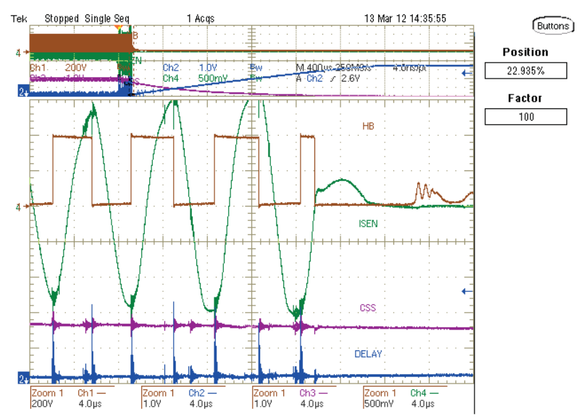

CH1: HB voltage CH2: DELAY
CH3: CSS CH4: ISEN
AM11629v1

Figure 28. Short-circuit - hiccup mode

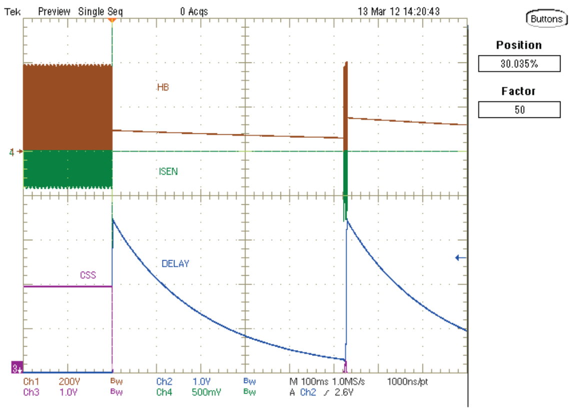

4.4 Anti-capacitive mode protection

The EVL6699-150W-SR demonstration board has been designed in such a way that the system does not work in capacitive mode during normal operation or failure conditions. As seen in *Figure 27*, even in dead short condition the LLC operates correctly in the inductive region, the same correct operation happens during load or input voltage transients.

Normally, the resonant half bridge converter operates with the resonant tank current lagging behind the square-wave voltage applied by the half bridge leg, like a circuit having a reactance of an inductive nature. In this way the applied voltage and the resonant current have the same sign at every transition of the half bridge, which is a necessary condition in order for soft-switching to occur (zero-voltage switching, ZVS at turn-on for both MOSFETs). Therefore, should the phase relationship reverse, i.e. the resonant tank current leads the applied voltage, such as in circuits having a capacitive reactance, soft-switching would be lost. This is termed capacitive mode operation and must be avoided because of its significant drawbacks:

1. Both MOSFETs feature hard-switching at turn-on, like in conventional PWM-controlled converters (see *Figure 14*). The associated capacitive losses may be considerably higher than the total power normally dissipated under “soft-switching” conditions and this may easily lead to their overheating, as heatsinking is not usually sized to handle this abnormal condition.
2. The body diode of the MOSFET just switched off conducts current during the deadtime and its voltage is abruptly reversed by the other MOSFET turned on (see *Figure 14*). Therefore, the conducting body diode (which does not generally have great reverse recovery characteristics) keeps its low impedance until it recovers, and so originating a condition equivalent to a shoot-through of the half bridge leg. This is a potentially destructive condition (see point 3) and causes additional power dissipation due to the current and voltage of the conducting body diode simultaneously high during part of its recovery.
3. There is an extremely high reverse dv/dt (many tens of V/ns!) experienced by the conducting body diode at the end of its recovery with the other MOSFET turned on. This dv/dt may exceed the rating of the MOSFET and lead to an immediate failure because of the second breakdown of the parasitic BJT intrinsic in its structure. If

a MOSFET is hot, the turn-on threshold of its parasitic BJT is lower, this dv/dt-induced failure is then far more likely.

4. When either MOSFET is turned on, the other one can be parasitically turned on too, if the current injected through its Cgd and flowing through the gate driver's pull-down is large enough to raise the gate voltage close to the turn-on threshold. This would be a lethal shoot-through condition for the half bridge leg.
5. The recovery of the body diodes generates large and energetic negative voltage spikes because of the unavoidable parasitic inductance of the PCB subject to its di/dt. These are coupled to the OUT pin and may damage the L6699.
6. There is a large common-mode EMI generation that adversely affects EMC.

Resonant converters work in capacitive mode when their switching frequency falls below a critical value that depends on the loading conditions and the input-to-output voltage ratio. They are especially prone to run in capacitive mode when the input voltage is lower than the minimum specified and/or the output is overloaded or short-circuited. Designing a converter so that it never works in capacitive mode, even under abnormal operating conditions, is certainly possible but this may pose unacceptable design constraints in some cases.

To prevent the severe drawbacks of capacitive mode operation, while enabling a design that needs to ensure Inductive mode operation only in the specified operating range, neglecting abnormal operating conditions, the L6699 provides the capacitive mode detection function.

The L6699 monitors the phase relationship between the tank current circuit sensed on the ISEN pin and the voltage applied to the tank circuit by the half bridge, checking that the former lags behind the latter (inductive mode operation). If the phase-shift approaches zero, which is indicative of impending capacitive mode operation, the monitoring circuit activates the anti-capacitive mode protection procedure so that the resulting frequency rise keeps the converter away from that dangerous condition. Also in this case, the DELAY pin is activated, so that the OLP function, if used, is eventually tripped, causing intermittent operation and reducing thermal stress.

If the phase relationship reverses abruptly (which may happen in the case of dead short at the converter output), the L6699 is stopped immediately, the soft-start capacitor CSS is totally discharged and a new soft-start cycle is initiated after 50 µs idle time. During this idle period the PFC_STOP pin is pulled low to stop the PFC stage as well.

5 Thermal map

In order to check the design reliability, a thermal mapping by means of an IR camera was done. Below, the thermal measurements of the board, component side, at nominal input voltage are shown. Some pointers, visible on the images, have been placed across key components or components showing high temperature. The ambient temperature during both measurements was 26 °C.

Figure 29. Thermal map at 115 V_{ac} - 60 Hz - full load

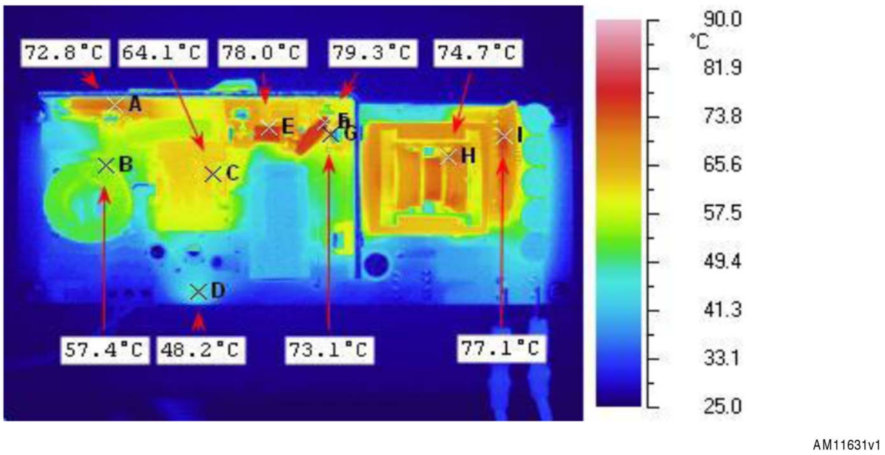

Figure 30. Thermal map at 230 V_{ac} - 50 Hz - full load

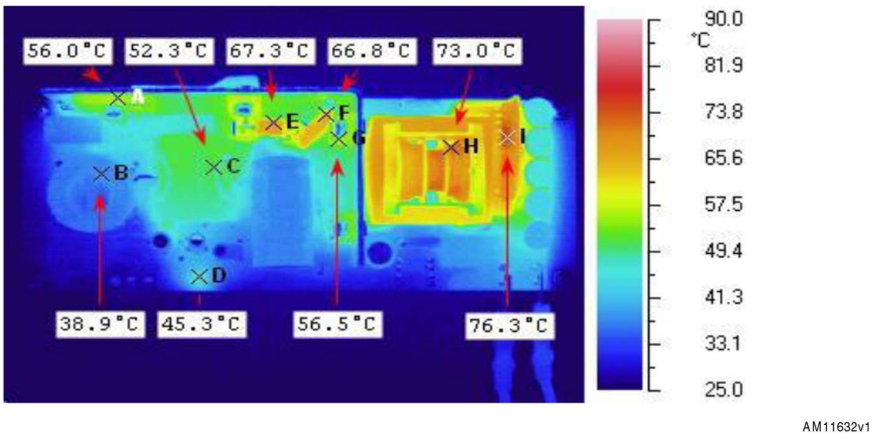

Table 6. Thermal maps reference points

Point	Reference	Description
A	D1	Bridge rectifier
B	L1	EMI filtering inductor
C	L2	PFC inductor
D	Q8	ICs supply regulator
E	D4	PFC output diode
F	R6	Inrush limiting NTC resistor
G	Q4	Resonant low-side MOSFET
H	T1	Resonant power transformer
I	Q501	SR MOSFET

6 Conducted emission pre-compliance test

The following figures represent the average measurement of the conducted emission at full load and nominal mains voltages. The EN55022 Class-B limit relevant to average measurements is indicated in red on the diagrams. In all test conditions the measurements are significantly below the limits.

Figure 31. CE average measurement at 115 V_{ac} - 60 Hz and full load

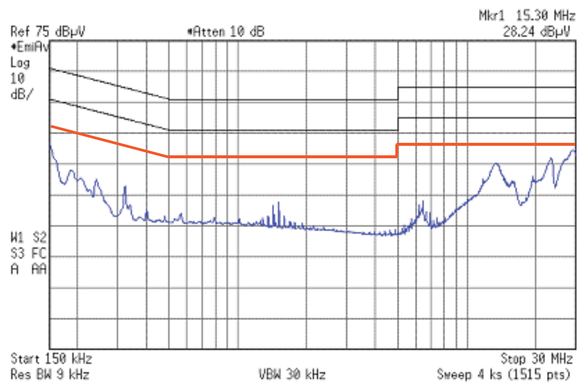

AM11633v1

Figure 32. CE average measurement at 230 V_{ac} - 50 Hz and full load

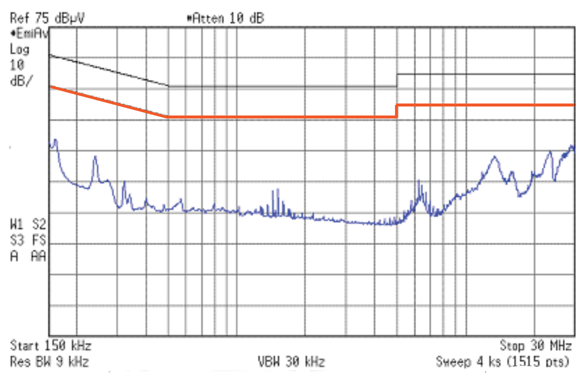

AM11634v1

7 Bill of material

Table 7. EVL6699-150W-SR demonstration board: motherboard bill of material

Des.	Part number / part value	Description	Supplier	Case
C1	470 nF - X2	X2 - film cap - B32922C3474K	EPCOS	9.0 × 18.0 p 15 mm
C2	2.2 nF - Y1	Y1 safety cap. CD12-E2GA222MYGSA	EPCOS	p10 mm
C3	2.2 nF - Y1	Y1 safety cap. CD12-E2GA222MYGSA	EPCOS	p10 mm
C4	470 nF - X2	X2 - film cap. B32922C3474K	EPCOS	9.0 × 18.0 p 15 mm
C5	470 nF - 520 V	520 V - film cap. - B32673Z5474K	EPCOS	7.0 x 26.5 p 22.5 mm
C6	330 nF	50 V CERCAP - general purpose	AVX	SMD 0805
C7	100 nF	100 V CERCAP - general purpose	AVX	PTH
C8	10 µF - 50 V	Aluminium Elcap - YXF series - 105 °C	Rubycon	Dia. 5.0 x 11 mm
C9	100 µF - 450 V	Aluminium Elcap - UPZ series - 105 °C	Nichicon	Dia. 18 x 32 mm
C10	1 nF	50 V CERCAP - general purpose	AVX	SMD 0805
C11	2.2 nF	50 V CERCAP - general purpose	AVX	SMD 0805
C12	1 µF	25 V CERCAP - general purpose	AVX	SMD 0805
C13	680 nF	25 V CERCAP - general purpose	AVX	SMD 1206
C14	68 nF	50 V CERCAP - general purpose	AVX	SMD 0805
C15	47 µF - 50 V	Aluminium Elcap - YXF series - 105 °C	Rubycon	Dia. 6.3 x 11 mm
C16	2.2 nF	50 V CERCAP - general purpose	AVX	SMD 1206
C17	330 pF	50 V - 5 % - C0G - CERCAP	AVX	SMD 0805
C18	4.7 µF	25 V CERCAP - general purpose	AVX	SMD 1206
C19	100 nF	50 V CERCAP - general purpose	AVX	SMD 1206
C20	2.2 nF - Y1	Y1 safety cap. CD12-E2GA222MYGSA	EPCOS	p10mm
C21	2.2 nF - Y1	Y1 safety cap. CD12-E2GA222MYGSA	EPCOS	p10mm
C22	220 pF	50 V CERCAP - general purpose	AVX	SMD 0805
C23	10 nF	50 V CERCAP - general purpose	AVX	SMD 0805
C24	220 µF - 50 V	Aluminium Elcap - YXF series - 105 °C	Rubycon	Dia. 10 x 16 mm
C25	1.5 nF	50 V CERCAP - general purpose	AVX	SMD 0805
C26	10 µF - 50 V	Aluminium Elcap - YXF series - 105 °C	Rubycon	Dia. 5.0 x 11 mm
C27	220 pF - 630 V	630 V CERCAP - GRM31A7U2J221JW31	Murata	SMD 1206
C28	22 nF	1 KV - film cap. B32652A223K	EPCOS	5.0 x 18.0 p 15 mm
C29	470 µF - 16 V	16 V OSCON CAP 16SEPC470M	Sanyo	Dia. 10 x 13 p 5 mm
C30	470 µF - 16 V	16 V OSCON CAP 16SEPC470M	Sanyo	Dia. 10 x 13 p 5 mm
C32	470 nF	50 V CERCAP - general purpose	AVX	SMD 0805
C33	1.5 nF	50 V CERCAP - general purpose	AVX	SMD 0805

Table 7. EVL6699-150W-SR demonstration board: motherboard bill of material (continued)

Des.	Part number / part value	Description	Supplier	Case
C34	100 nF	50 V CERCAP - general purpose	AVX	SMD 0805
C36	1 µF - 50 V	50 V CERCAP - general purpose	AVX	SMD 1206
C37	470 µF-16 V	16 V OSCON CAP 16SEPC470M	Sanyo	Dia. 10 x 13 p 5 mm
C38	100 nF	50 V CERCAP - general purpose	AVX	SMD 0805
C39	100 nF	50 V CERCAP - general purpose	AVX	SMD 0805
C40	100 nF	50 V CERCAP - general purpose	AVX	SMD 1206
C42	100 nF	50 V CERCAP - general purpose	AVX	SMD 0805
C43	4.7 nF	50 V CERCAP - general purpose	AVX	SMD 0805
C44	1.5 nF	50 V CERCAP - general purpose	AVX	SMD 0805
C45	220 nF	25 V CERCAP - general purpose	AVX	SMD 0805
C47	1 nF	50 V CERCAP - general purpose	AVX	SMD 0805
C48	1 nF	50 V CERCAP - general purpose	AVX	SMD 0805
C49	470 µF-16 V	16 V OSCON CAP 16SEPC470M	Sanyo	Dia. 10 x 13 p 5 mm
C50	470 µF-16 V	16 V OSCON CAP 16SEPC470M	Sanyo	Dia. 10 x 13 p 5 mm
C51	100 nF	50 V CERCAP - general purpose	AVX	SMD 0805
C52	1 nF	25 V CERCAP - general purpose	AVX	SMD 0805
D1	GBU8J	Single-phase bridge rectifier	Vishay	STYLE GBU
D2	LL4148	High speed signal diode	Vishay	Mini Melf SOD-80
D3	1N4005	General purpose rectifier	Vishay	DO-41
D4	STTH5L06	Ultrafast high-voltage rectifier	ST	DO-201
D5	LL4148	High speed signal diode	Vishay	Mini Melf SOD-80
D6	LL4148	High speed signal diode	Vishay	Mini Melf SOD-80
D7	STPS140Z	Power Schottky rectifier	ST	SOD-123
D9	STPS2H100A	Power Schottky diode	ST	SMB
D12	BZV55-C43	Zener diode	Vishay	Mini Melf SOD-80
D14	LL4148	High speed signal diode	Vishay	Mini Melf SOD-80
D17	LL4148	High speed signal diode	Vishay	Mini Melf SOD-80
D18	LL4148	High speed signal diode	Vishay	Mini Melf SOD-80
D19	LL4148	High speed signal diode	Vishay	Mini Melf SOD-80
D20	BZV55-B15	Zener diode	Vishay	Mini Melf SOD-80
D21	LL4148	High speed signal diode	Vishay	Mini Melf SOD-80
F1	FUSE T4A	Fuse 4 A - time lag - 3921400	Littlefuse	8.5 x 4 p. 5.08 mm
HS1	HEAT-SINK	Heatsink for D1, Q1, Q3, Q4		DWG

Table 7. EVL6699-150W-SR demonstration board: motherboard bill of material (continued)

Des.	Part number / part value	Description	Supplier	Case
J1	MKDS 1,5/ 3-5,08	PCB term. block, screw conn., pitch 5 mm - 3 W	Phoenix Contact	DWG
J2	FASTON	FASTON - connector		DWG
J3	FASTON	FASTON - connector		DWG
JPX1	JUMPER	Bare copper wire jumper		DWG
L1	2019.0002	Common mode choke - EMI filter	Magnetica	DWG
L2	1975.0004	PFC inductor - 0.31 mH - PQ26/25	Magnetica	DWG
Q1	STF21N65M5	N-channel Power MOSFET	ST	TO-220FP
Q2	BC857C	PNP small signal BJT	Vishay	SOT-23
Q3	STF8NM50N	N-channel Power MOSFET	ST	TO-220FP
Q4	STF8NM50N	N-channel Power MOSFET	ST	TO-220FP
Q8	BC847C	NPN small signal BJT	Vishay	SOT-23
Q9	BC847C	NPN small signal BJT	Vishay	SOT-23
R1	6.8 MΩ	SMD STD film res. - 1/4 W - 5% - 250 ppm/°C	Vishay	SMD 1206
R2	5.6 MΩ	SMD STD film res. - 1/4 W - 5% - 250 ppm/°C	Vishay	SMD 1206
R3	2.2 MΩ	SMD STD film res. - 1/4 W - 1% - 100 ppm/°C	Vishay	SMD 1206
R5	75 Ω	SMD STD film res. - 1/4 W - 5% - 250 ppm/°C	Vishay	SMD 1206
R6	NTC 2R5-S237	NTC resistor B57237S0259M000	EPCOS	DWG
R7	2.2 MΩ	SMD STD film res. - 1/4 W - 1% - 100 ppm/°C	Vishay	SMD 1206
R8	2.2 MΩ	SMD STD film res. - 1/4 W - 1% - 100 ppm/°C	Vishay	SMD 1206
R9	160 KΩ	SMD STD film res. - 1/8 W - 1% - 100 ppm/°C	Vishay	SMD 0805
R10	56 KΩ	SMD STD film res. - 1/8 W - 1% - 100 ppm/°C	Vishay	SMD 0805
R11	2.2 MΩ	SMD STD film res. - 1/4 W - 1% - 100 ppm/°C	Vishay	SMD 1206
R12	2.2 MΩ	SMD STD film res. - 1/4 W - 1% - 100 ppm/°C	Vishay	SMD 1206
R13	9.1 KΩ	SMD STD film res. - 1/4 W - 1% - 100 ppm/°C	Vishay	SMD 1206
R14	100 KΩ	SMD STD film res. - 1/8 W - 5% - 250 ppm/°C	Vishay	SMD 0805
R15	56 KΩ	SMD STD film res. - 1/4 W - 1% - 100 ppm/°C	Vishay	SMD 1206
R16	2.7 KΩ	SMD STD film res. - 1/8 W - 5% - 250 ppm/°C	Vishay	SMD 0805
R17	2.2 MΩ	SMD STD film res. - 1/4 W - 1% - 100 ppm/°C	Vishay	SMD 1206
R18	82 KΩ	SMD STD film res. - 1/8 W - 5% - 250 ppm/°C	Vishay	SMD 0805
R19	56 KΩ	SMD STD film res. - 1/8 W - 5% - 250 ppm/°C	Vishay	SMD 0805
R20	33 Ω	SMD STD film res. - 1/8 W - 5% - 250 ppm/°C	Vishay	SMD 0805
R21	22 Ω	SMD STD film res. - 1/8 W - 5% - 250 ppm/°C	Vishay	SMD 0805
R22	0.22 Ω	RSMF1TB - metal film res. - 1 W - 2% - 250 ppm/°C	AKANEOHM	PTH

Table 7. EVL6699-150W-SR demonstration board: motherboard bill of material (continued)

Des.	Part number / part value	Description	Supplier	Case
R23	0.22 Ω	RSMF1TB - metal film res. - 1 W - 2% - 250 ppm/°C	AKANEOHM	PTH
R24	1 MΩ	SMD STD film res. - 1/8 W - 5% - 250 ppm/°C	Vishay	SMD 0805
R25	56 Ω	SMD STD film res. - 1/8 W - 5% - 250 ppm/°C	Vishay	SMD 0805
R26	1 MΩ	SMD STD film res. - 1/8 W - 1% - 100 ppm/°C	Vishay	SMD 0805
R27	470 Ω	SMD STD film res. - 1/4 W - 5% - 250 ppm/°C	Vishay	SMD 1206
R28	33 KΩ	SMD STD film res. - 1/8 W - 1% - 100 ppm/°C	Vishay	SMD 0805
R29	1 KΩ	SMD STD film res. - 1/4 W - 5% - 250 ppm/°C	Vishay	SMD 1206
R30	10 Ω	SMD STD film res. - 1/8 W - 5% - 250 ppm/°C	Vishay	SMD 0805
R31	20 KΩ	SMD STD film res. - 1/8 W - 1% - 100 ppm/°C	Vishay	SMD 0805
R32	47 Ω	SMD STD film res. - 1/8 W - 5% - 250ppm/°C	Vishay	SMD 0805
R34	8.2 KΩ	SMD STD film res. - 1/8 W - 1% - 100 ppm/°C	Vishay	SMD 0805
R35	180 KΩ	SMD STD film res. - 1/8 W - 1% - 100 ppm/°C	Vishay	SMD 0805
R36	1.8 MΩ	SMD STD film res. - 1/8 W - 5% - 250 ppm/°C	Vishay	SMD 0805
R37	220 KΩ	SMD STD film res. - 1/4 W - 5% - 250 ppm/°C	Vishay	SMD 1206
R38	56 Ω	SMD STD film res. - 1/8 W - 5% - 250 ppm/°C	Vishay	SMD 0805
R40	68 Ω	SMD STD film res. - 1/4 W - 5% - 250 ppm/°C	Vishay	SMD 1206
R41	100 Ω	SFR25 axial stand. Film res. - 0.4 W - 5% - 250 ppm/°C	Vishay	PTH
R42	1 KΩ	SMD STD film res. - 1/8 W - 5% - 250 ppm/°C	Vishay	SMD 0805
R43	51 Ω	SMD STD film res. - 1/8 W - 5% - 250 ppm/°C	Vishay	SMD 0805
R44	6.3 KΩ	SMD STD film res. - 1/4 W - 5% - 250 ppm/°C	Vishay	SMD 1206
R45	3.3 Ω	SMD STD film res. - 1/8 W - 5% - 250 ppm/°C	Vishay	SMD 0805
R46	100 KΩ	SMD STD film res. - 1/8 W - 5% - 250 ppm/°C	Vishay	SMD 0805
R48	47 KΩ	SMD STD film res. - 1/8 W - 5% - 250 ppm/°C	Vishay	SMD 0805
R49	91 KΩ	SMD STD film res. - 1/8 W - 1% - 100 ppm/°C	Vishay	SMD 1206
R50	12 KΩ	SMD STD film res. - 1/8 W - 1% - 100 ppm/°C	Vishay	SMD 0805
R51	91 KΩ	SMD STD film res. - 1/8 W - 1% - 100 ppm/°C	Vishay	SMD 0805
R52	1.5 KΩ	SMD STD film res. - 1/8 W - 1% - 100 ppm/°C	Vishay	SMD 0805
R53	2.2 KΩ	SMD STD film res. - 1/8 W - 1% - 100 ppm/°C	Vishay	SMD 0805
R54	0 Ω	SMD STD film res. - 1/8 W - 5% - 250 ppm/°C	Vishay	SMD 0805
R55	2.7 KΩ	SMD STD film res. - 1/8 W - 1% - 100 ppm/°C	Vishay	SMD 0805
R57	0.02 Ω	SMD current sense resistor - ERJM1WTF2M0U	Panasonic	SMD 2512
R58	100 KΩ	SMD STD film res. - 1/8 W - 5% - 250 ppm/°C	Vishay	SMD 0805
R59	100 KΩ	SMD STD film res. - 1/8 W - 5% - 250 ppm/°C	Vishay	SMD 0805

Table 7. EVL6699-150W-SR demonstration board: motherboard bill of material (continued)

Des.	Part number / part value	Description	Supplier	Case
R60	10 KΩ	SMD STD film res. - 1/8 W - 5% - 250 ppm/°C	Vishay	SMD 0805
R63	0 Ω	SMD STD film res. - 1/8 W - 5% - 250 ppm/°C	Vishay	SMD 0805
R64	10 MΩ	SMD STD film res. - 1/8 W - 5% - 250 ppm/°C	Vishay	SMD 0805
R68	5.6 KΩ	SMD STD film res. - 1/8 W - 5% - 250 ppm/°C	Vishay	SMD 0805
R69	24 KΩ	SMD STD film res. - 1/8 W - 5% - 250 ppm/°C	Vishay	SMD 0805
R70	22 KΩ	SMD STD film res. - 1/8 W - 1% - 100 ppm/°C	Vishay	SMD 0805
R71	1 KΩ	SMD STD film res. - 1/8 W - 5% - 250 ppm/°C	Vishay	SMD 1206
R72	68 KΩ	SMD STD film res. - 1/8 W - 1% - 100 ppm/°C	Vishay	SMD 0805
R73	22 Ω	SMD STD film res. - 1/8 W - 5% - 250 ppm/°C	Vishay	SMD 0805
R75	0 Ω	SMD STD film res. - 1/8 W - 5% - 250 ppm/°C	Vishay	SMD 0805
R76	33 KΩ	SMD STD film res. - 1/8 W - 5% - 250 ppm/°C	Vishay	SMD 0805
R77	1 KΩ	SMD STD film res. - 1/8 W - 5% - 250 ppm/°C	Vishay	SMD 0805
R78	33 Ω	SMD STD film res. - 1/4 W - 5% - 250 ppm/°C	Vishay	SMD 1206
R79	270 Ω	SMD STD film res. - 1/4 W - 5% - 250 ppm/°C	Vishay	SMD 1206
T1	1860.0069	Resonant power transformer	Magnetica	ETD34
U1	L6563H	High-voltage startup TM PFC controller	ST	SO-16
U2	L6699D	Improved HV resonant controller	ST	SO-16

Table 8. EVL6699-150W-SR demonstration board: daughterboard bill of material

Des.	Part number/ part value	Description	Supplier	Case
C501	4.7 nF	50 V CERCAP - general purpose	Vishay	SMD 0805
C502	100 nF	50 V CERCAP - general purpose	Vishay	SMD 0805
C503	1 µF	50 V CERCAP - general purpose	Vishay	SMD 0805
C504	150 pF	50 V CERCAP - general purpose	Vishay	SMD 0805
C505	150 pF	50 V CERCAP - general purpose	Vishay	SMD 0805
D501	BAS316	Fast switching signal diode	ST	SOD-123
D502	BAS316	Fast switching signal diode	ST	SOD-123
JP501	HEADER 13	13-pin connector		
Q501	STL140N4LLF5	N-channel Power MOSFET	ST	PowerFLAT™
Q502	STL140N4LLF5	N-channel Power MOSFET	ST	PowerFLAT™
R501	10 Ω	SMD STD film res. - 1/8 W - 5% - 250 ppm/°C	Vishay	SMD 0805
R502	10 Ω	SMD STD film res. - 1/8 W - 5% - 250 ppm/°C	Vishay	SMD 0805
R503	10 Ω	SMD STD film res. - 1/8 W - 5% - 250 ppm/°C	Vishay	SMD 0805

Table 8. EVL6699-150W-SR demonstration board: daughterboard bill of material (continued)

Des.	Part number/ part value	Description	Supplier	Case
R504	150 kΩ	SMD STD film res. - 1/8 W - 1% - 100 ppm/°C	Vishay	SMD 0805
R505	33 kΩ	SMD STD film res. - 1/8 W - 1% - 100 ppm/°C	Vishay	SMD 0805
R506	330 Ω	SMD STD film res. - 1/8 W - 5% - 250 ppm/°C	Vishay	SMD 0805
R507	330 Ω	SMD STD film res. - 1/8 W - 5% - 250 ppm/°C	Vishay	SMD 0805
RX1	0 Ω	SMD STD film res. - 1/8 W - 5% - 250 ppm/°C	Vishay	SMD 0805
U501	SRK2000A	SR smart driver for LLC resonant converter	ST	SO8

8 PFC coil specification

8.1 General description and characteristics

- Application type: consumer, home appliance
- Transformer type: open
- Coil former: vertical type, 6 + 6 pins
- Max. temp. rise: 45 °C
- Max. operating ambient temperature: 60 °C
- Mains insulation: n.a.
- Unit finishing: varnished.

8.2 Electrical characteristics

- Converter topology: boost, transition mode
- Core type: PQ26/25-PC44 or equivalent
- Min. operating frequency: 40 kHz
- Typical operating frequency: 120 kHz
- Primary inductance: 310 µH ± 10% at 1 kHz - 0.25 V [a]
- Peak current: 5.6 Apk.

8.3 Electrical diagram and winding characteristics

Figure 33. PFC coil electrical diagram

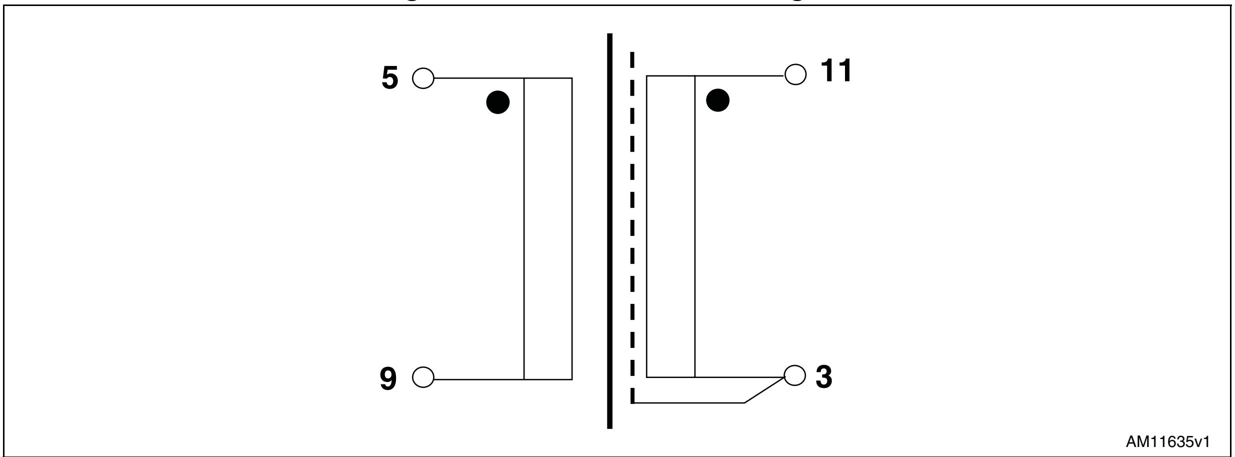

a. Measured between pins #5 and #9.

Table 9. PFC coil winding data

Pins	Windings	RMS current	Number of turns	Wire type
11 - 3	AUX	0.05 A_{RMS}	5	ϕ 0.28 mm – G2
5 - 9	Primary	2.3 A_{RMS}	50	50xϕ 0.1 mm – G1

8.4 Mechanical aspect and pin numbering

- Maximum height from PCB: 30 mm
- Coil former type: vertical, 6 + 6 pins (pins 1, 2, 4, 6, 7, 10, 12 are removed)
- Pin distance: 3.81 mm
- Row distance: 25.4 mm
- External copper shield: not insulated, wound around the ferrite core and including the coil former. Height is 8 mm. Connected to pin #3 by a soldered solid wire.

Figure 34. PFC coil mechanical aspect

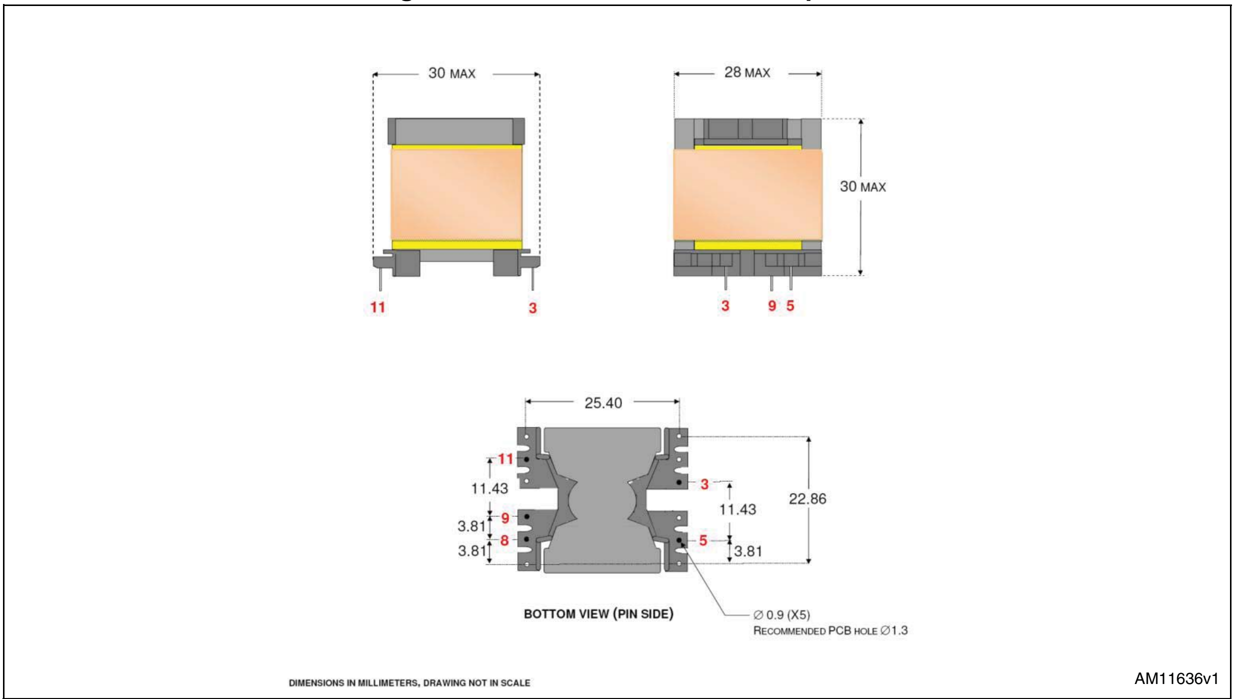

8.5 Manufacturer

- Magnetica - Italy
- Inductor P/N: 1975.0004.

9 Transformer specifications

9.1 General description and characteristics

- Application type: consumer, home appliance
- Transformer type: open
- Coil former: horizontal type, 7 + 7 pins, two slots
- Max. temp. rise: 45 °C
- Max. operating ambient temperature: 60 °C
- Mains insulation: acc. to EN60065.

9.2 Electrical characteristics

- Converter topology: half bridge, resonant
- Core Type: ETD34-PC44 or equivalent
- Min. operating frequency: 60 kHz
- Typical operating frequency: 100k Hz
- Primary inductance: 1000 µH ± 10% at 1 kHz - 0.25 V[(b)]
- Leakage inductance: 100 µH ± 10% at 100 kHz - 0.25 V[(c)].

9.3 Electrical diagram and winding characteristics

Figure 35. Transformer electrical diagram

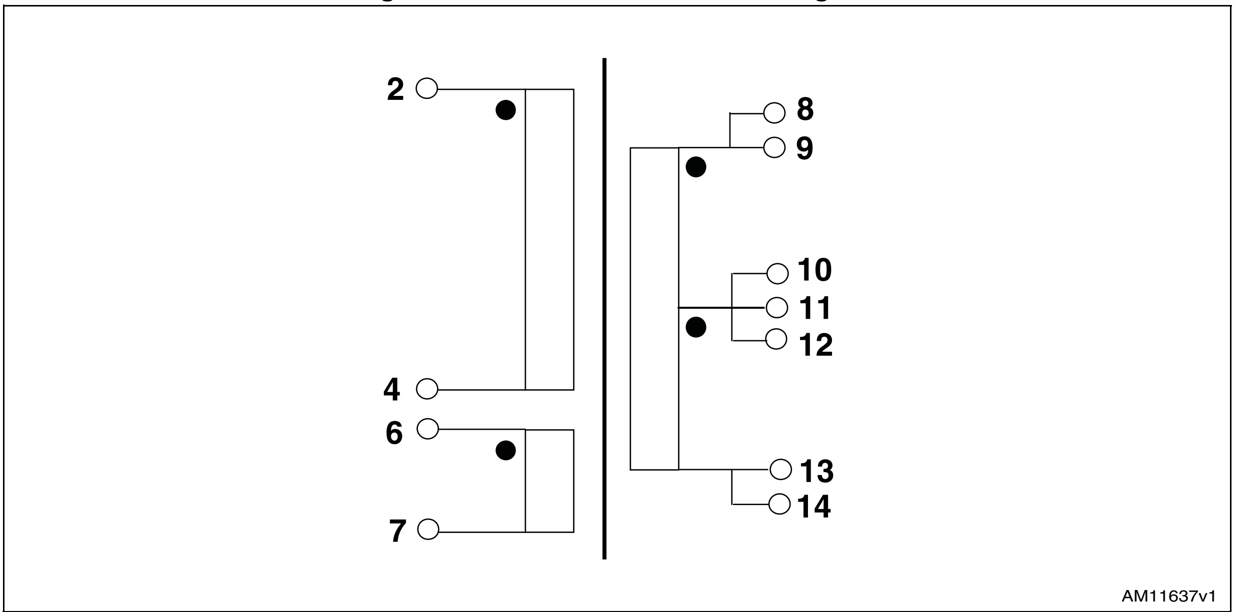

b. Measured between pins 2 - 4.

c. Measured between pins 2 - 4 with only half secondary winding shorted at a time.

Table 10. Transformer winding data

Pins	Winding	RMS current	Number of turns	Wire type
2 - 4	Primary	1 A_{RMS}	34	30 x ∅ 0.1 mm – G1
8 - 11	SEC-1A(1)	8.5 A_{RMS}	2	90 x ∅ 0.1 mm – G1
9 - 10	SEC-1B(1)	8.5 A_{RMS}	2	90 x ∅ 0.1 mm – G1
10 - 13	SEC-2A(1)	8.5 A_{RMS}	2	90 x ∅ 0.1 mm – G1
12 - 14	SEC-2B(1)	8.5 A_{RMS}	2	90 x ∅ 0.1 mm – G1
6 - 7	AUX(2)	0.05 A_{RMS}	3	∅ 0.28 mm – G2

1. Secondary windings A and B are in parallel.
2. Aux winding is wound on top of primary winding.

9.4 Mechanical aspect and pin numbering

- Maximum height from PCB: 30 mm
- Coil former type: horizontal, 7 + 7 pins (pins #3 and #5 are removed)
- Pin distance: 5.08 mm
- Row distance: 25.4 mm.

Figure 36. Transformer overall drawing

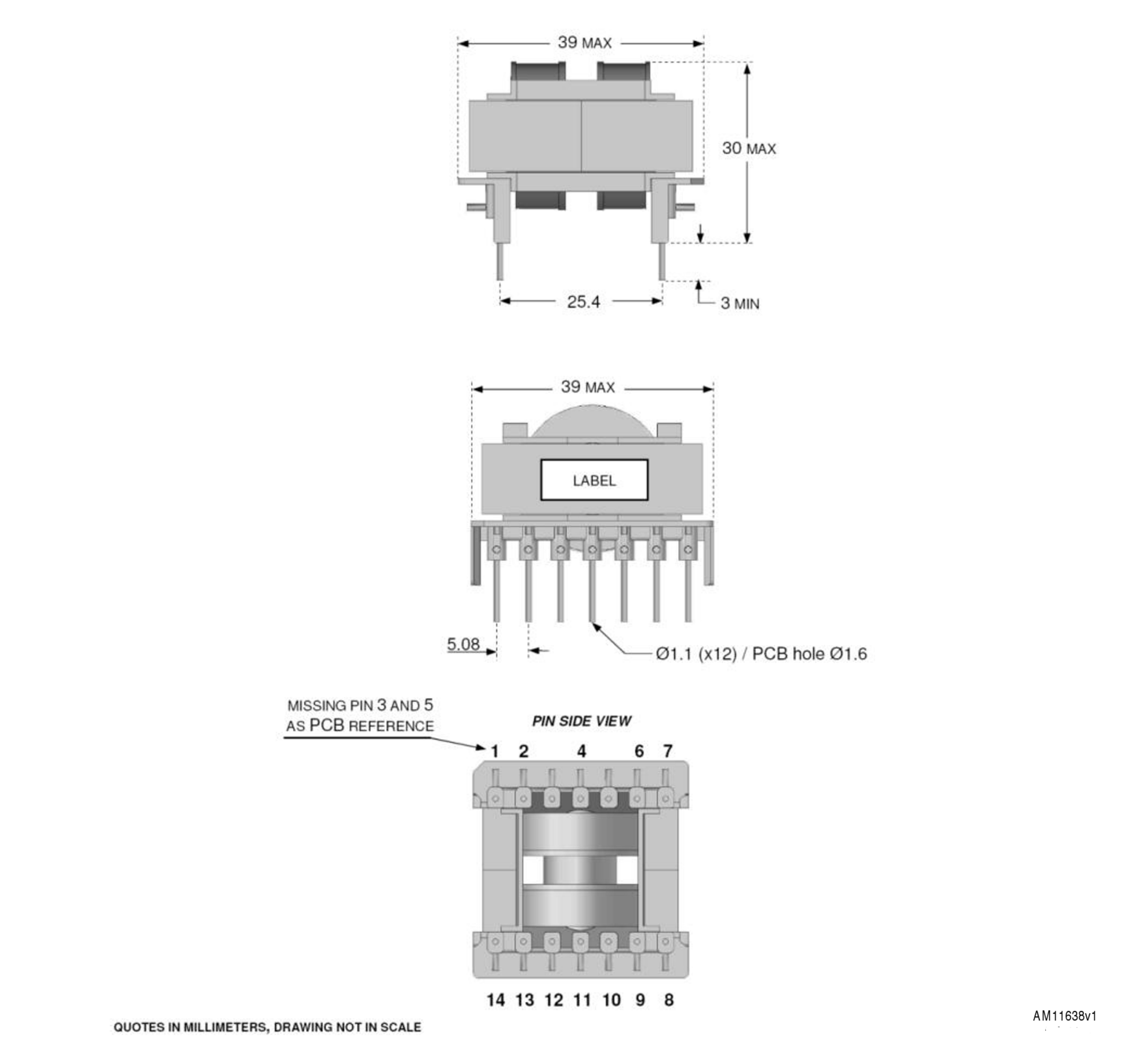

9.5 Manufacturer

- Magnetica - Italy
- Transformer P/N: 1860.0069.

10 Revision history

Table 11. Document revision history

Date	Revision	Changes
19-Jul-2012	1	Initial release.
18-Apr-2013	2	Updated *Table 8: EVL6699-150W-SR demonstration board: daughterboard bill of material*.
07-Apr-2014	3	Replaced “SRK2000” by “SRK2000A” in main title *12 V - 150 W resonant converter with synchronous rectification using the L6563H, L6699 and SRK2000A on page 1*, *Section 1 on page 6*, *Section 4 on page 18*, and *Section 7 on page 29*. Updated *Section : Introduction on page 1*. Updated *Table 1 on page 6* (updated “Parameters” and “Values”). Updated *Figure 2 on page 8* (replaced by new figure). Updated *Equation 2 on page 8* (updated *Equation 2* and text above). Updated *Equation 3 on page 9* (updated *Equation 3* and text below). Updated *Figure 3 on page 12* (updated R72, Q1, and U501 parts, minor modifications). Updated *Table 2 on page 13* (updated “Pin” rows of “No load”, added rows with 10% load conditions). Updated *Figure 4 on page 13* (replaced by new figure). Updated *Table 3 on page 14* (updated title, header, added “Efficiency at 10% load” row, updated limits of “No load input power”). Updated *Table 7 on page 29* (updated “Part number/part value” of “C18”, updated units throughout *Table 7*). Updated *Table 8 on page 33* (updated “Description” of “C27”, “C29”, “C30”, “C37”, “C49”, “C50”, “Part number/part value” of “R72” and “U501” items, updated units throughout *Table 8*). Minor modifications throughout document.